Muon g-2 and thermal DM with $U(1)_{L_\mu - L_\tau}$ gauge symmetry : Revisited

Pyungwon Ko (KIAS)

With Seungwon Baek, Jongkuk Kim
(in preparation)

CAU 2022 BSM Workshop
Feb. 7-10 (2022)

Contents

- SM + $U(1)_{L_\mu - L_\tau}$ gauge symmetry
- Muon g-2 and constraints
- $U(1)_{L_\mu - L_\tau}$ - charged DM : Z' only vs. $Z' + \phi$
- Roles of $U(1)_{L_\mu - L_\tau}$ breaking scalar ϕ
- DM phenomenology with $Z' + \phi$ (generic, Z_2 , Z_3 cases)
- Conclusion

SM+$U(1)_{L_\mu - L_\tau}$ gauge sym

- He, Josh, Lew, Volkas, PRD 43, 22; PRD 44, 2118 (1991)
- One of the anomaly free gauge groups without extension of fermion contents
- The simplest anomaly free U(1) extensions that couple to the SM fermions directly
- Can affect the muon g-2, PAMELA e^+ excess, (and B anomalies with extra fermions : Not covered in this talk)

Muon g-2

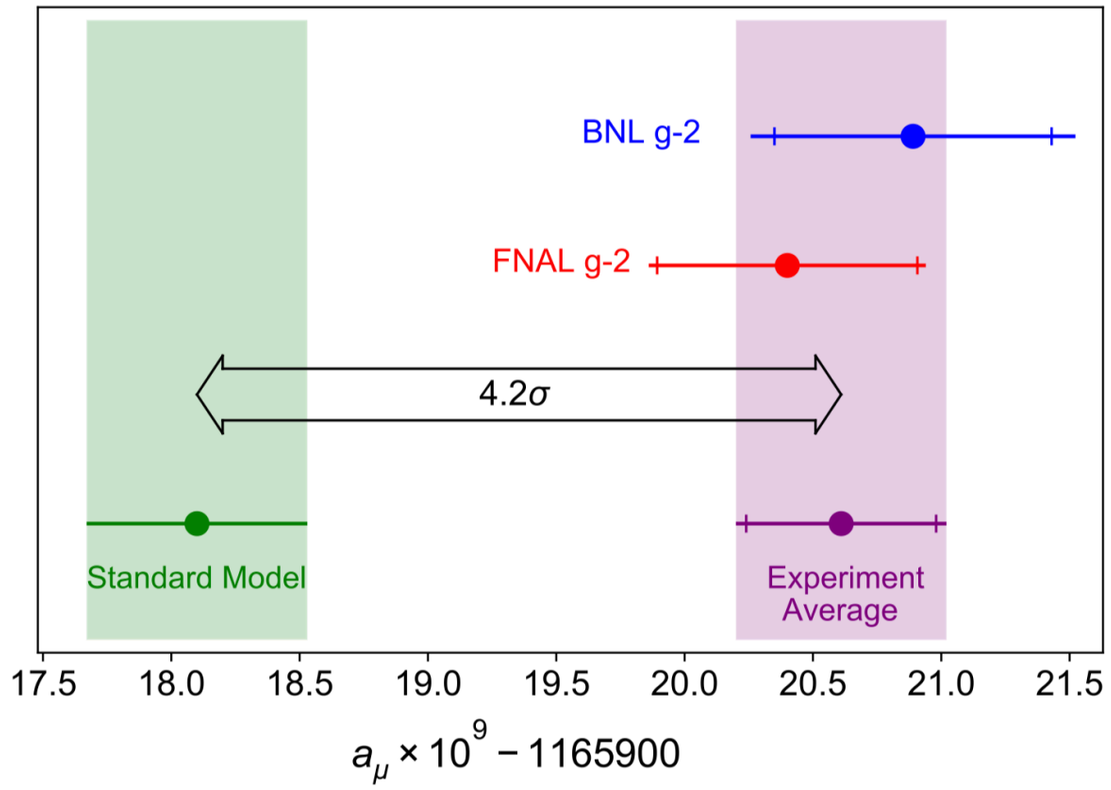

The Muon g-2 Collaboration, 2104.03281

Excellent example for graduate students

- **Relativistic E&M (spinning particle in EM fields)**
- **Special relativity (time dilation)**
- **(V-A) structure of charged weak interaction**

Muon (g-2) in $U(1)_{\mu-\tau}$ Model

Baek, Deshpande, He, Ko : hep-ph/0104141
Baek, Ko : arXiv:0811.1646 [hep-ph]

$$\begin{array}{ll} L_L^e: (1,2,-1)(0) & e_R: (1,1,-2)(0) \\ L_L^\mu: (1,2,-1)(2a) & \mu_R: (1,1,-2)(2a) \\ L_L^\tau: (1,2,-1)(-2a) & \mu_R: (1,1,-2)(-2a). \end{array}$$

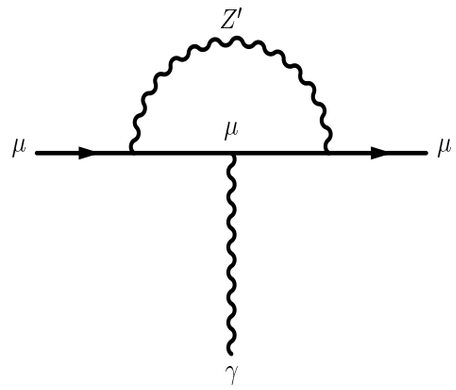

$$\Delta a_\mu = \frac{\alpha'}{2\pi}\int_0^1 dx \frac{2m_\mu^2 x^2(1-x)}{x^2 m_\mu^2 + (1-x)M_{Z'}^2} \approx \frac{\alpha'}{2\pi}\frac{2m_\mu^2}{3M_{Z'}^2}$$

$$Z' \to \mu^+\mu^-, \tau^+\tau^-, \nu_\alpha\bar{\nu}_\alpha \text{ (with } \alpha = \mu \text{ or } \tau), \ \psi_D\overline{\psi}_D$$

$\Gamma(Z' \to \mu^+\mu^-) = \Gamma(Z' \to \tau^+\tau^-) = 2\Gamma(Z' \to \nu_\mu\bar{\nu}_\mu) = 2\Gamma(Z' \to \nu_\tau\bar{\nu}_\tau) = \Gamma(Z' \to \psi_D\bar{\psi}_D)$

if $M_{Z'} \gg m_\mu, m_\tau, M_{\rm DM}$. The total decay rate of Z' is approximately given by

$$\Gamma_{\rm tot}(Z') = \frac{\alpha'}{3} M_{Z'} \times 4(3) \approx \frac{4(\text{or } 3)}{3} \text{ GeV} \left(\frac{\alpha'}{10^{-2}}\right) \left(\frac{M_{Z'}}{100\text{GeV}}\right)$$

$$\begin{aligned} q\bar{q} \text{ (or } e^+e^-) &\to \gamma^*, Z^* \to \mu^+\mu^- Z', \tau^+\tau^- Z' \\ &\to Z^* \to \nu_\mu\bar{\nu}_\mu Z', \nu_\tau\bar{\nu}_\tau Z' \end{aligned}$$

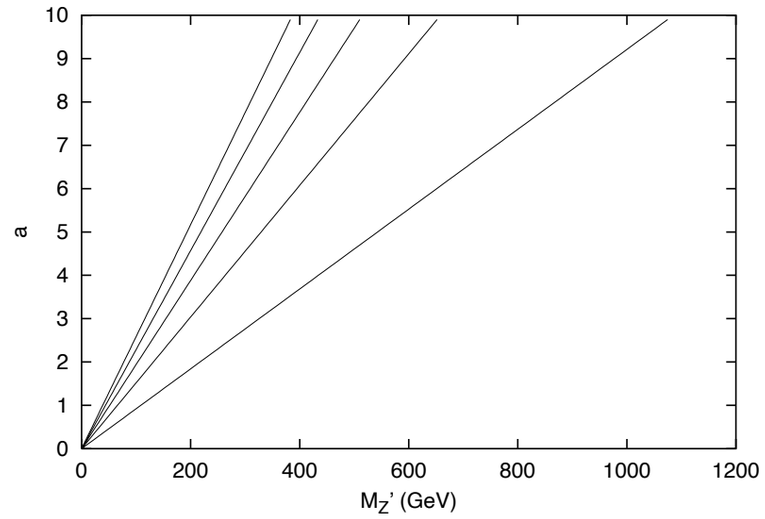

FIG. 2. Δa_μ on the a vs. $m_{Z'}$ plane in case b). The lines from left to right are for Δa_μ away from its central value at $+2\sigma, +1\sigma, 0, -1\sigma$ and -2σ, respectively.

Baek and Ko, arXiv:0811.1646, for PAMELA e^+ excess

$$\mathcal{L}_{\rm Model} = \mathcal{L}_{\rm SM} + \mathcal{L}_{\rm New}$$

$$\mathcal{L}_{\rm New} = -\frac{1}{4} Z'_{\mu\nu} Z'^{\mu\nu} + \overline{\psi_D} i D\cdot\gamma \psi_D - M_{\psi_D}\overline{\psi_D}\psi_D + D_\mu \phi^* D^\mu \phi$$
$$-\lambda_\phi (\phi^*\phi)^2 - \mu_\phi^2 \phi^*\phi - \lambda_{H\phi}\phi^*\phi H^\dagger H.$$

Here we ignored kinetic mixing for simplicity

$$D_\mu = \partial_\mu + ieQA_\mu + i\frac{e}{s_W c_S}(I_3 - s_W^2 Q)Z_\mu + ig' Y' Z'_\mu$$

muon g-2, Leptophilc DM, Collider Signature

Muon (g-2)

$$\Delta a_\mu = a_\mu^{\rm exp} - a_\mu^{\rm SM} = (302 \pm 88) \times 10^{-11}.$$

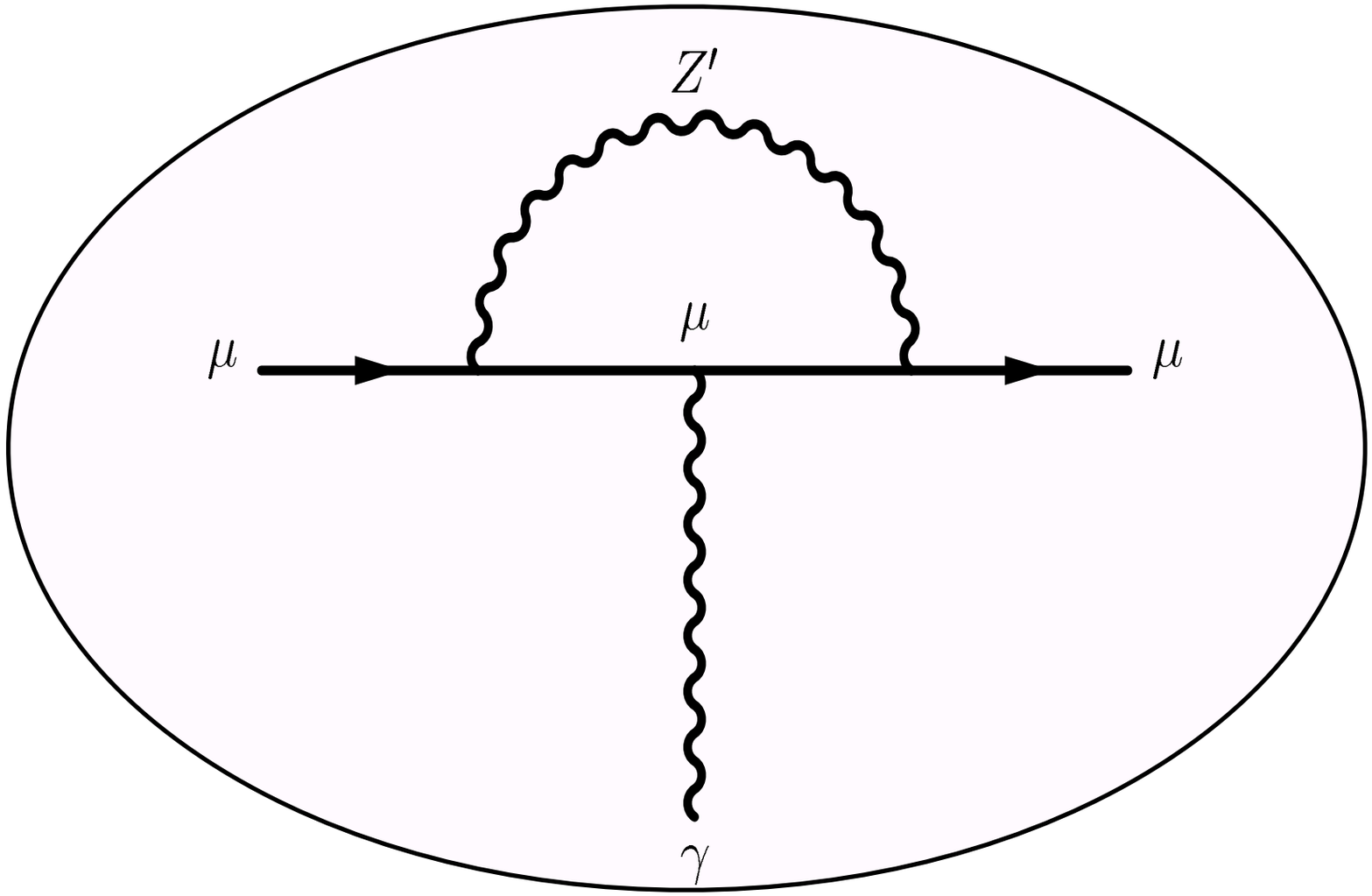

$$\Delta a_\mu = \frac{\alpha^{'}}{2\pi} \int_0^1 dx \frac{2m_\mu^2 x^2(1-x)}{x^2 m_\mu^2 + (1-x) M_{Z'}^2} \approx \frac{\alpha^{'}}{2\pi} \frac{2m_\mu^2}{3M_{Z'}^2}$$

Collider Signatures

$$Z^{'} \to \mu^+\mu^-, \tau^+\tau^-, \nu_\alpha\bar{\nu}_\alpha \text{ (with } \alpha = \mu \text{ or } \tau), \ \psi_D\overline{\psi}_D \ ,$$

$$\Gamma(Z^{'} \to \mu^+\mu^-) = \Gamma(Z^{'} \to \tau^+\tau^-) = 2\Gamma(Z^{'} \to \nu_\mu\bar{\nu}_\mu) = 2\Gamma(Z^{'} \to \nu_\tau\bar{\nu}_\tau) = \Gamma(Z^{'} \to \psi_D\bar{\psi}_D)$$

$$\Gamma_{\rm tot}(Z^{'}) = \frac{\alpha^{'}}{3}\ M_{Z^{'}} \times 4(3) \approx \frac{4(\text{or } 3)}{3}\ \text{GeV}\ \left(\frac{\alpha^{'}}{10^{-2}}\right)\ \left(\frac{M_{Z^{'}}}{100\text{GeV}}\right)$$

The dominant mechanisms of $Z^{'}$ productions at available colliders are

$$\begin{aligned} q\bar{q} \text{ (or } e^+e^-) &\to \gamma^*, Z^* \to \mu^+\mu^- Z^{'}, \tau^+\tau^- Z^{'} \\ &\to Z^* \to \nu_\mu\bar{\nu}_\mu Z^{'}, \nu_\tau\nu_\tau Z^{'} \end{aligned}$$

There are also vector boson fusion processes such as

$$\begin{aligned} W^+W^- &\to \nu_\mu\bar{\nu}_\mu Z^{'} \ \ (\text{or } \mu^+\mu^-\text{Z}^{'}), \quad \text{etc.} \\ Z^0Z^0 &\to \nu_\mu\bar{\nu}_\mu Z^{'} \ \ (\text{or } \mu^+\mu^-\text{Z}^{'}), \quad \text{etc.} \\ W^+Z^0 &\to \nu_\mu\bar{\mu} Z^{'} \ \ (\text{or } \mu^+\mu^-\text{Z}^{'}), \quad \text{etc.} \end{aligned}$$

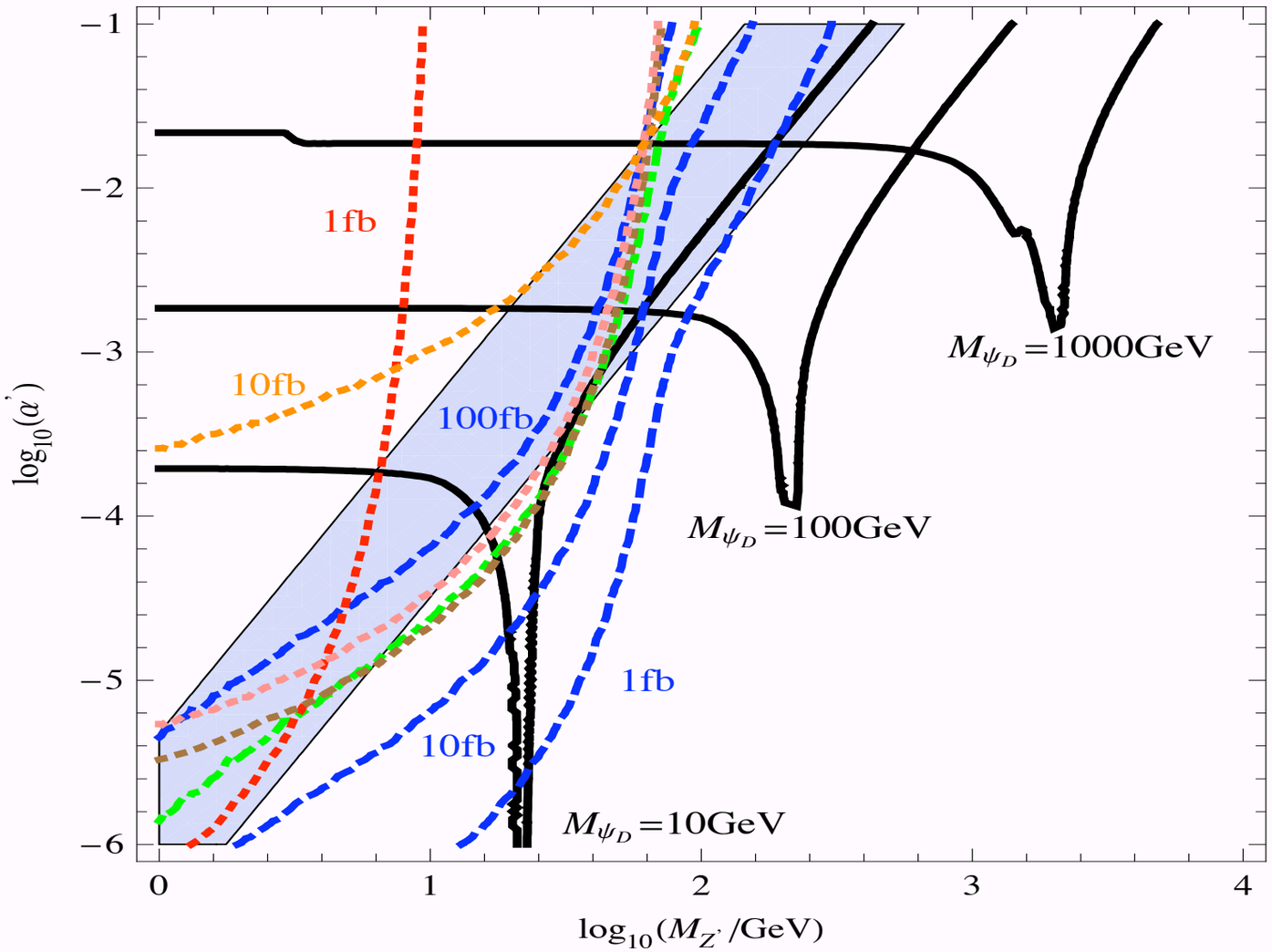

Figure 1: The relic density of CDM (black), the muon $(g-2)_\mu$ (blue band), the production cross section at B factories (1 fb, red dotted), Tevatron (10 fb, green dotdashed), LEP (10 fb, pink dotted), LEP2 (10 fb, orange dotted), LHC (1 fb, 10 fb, 100 fb, blue dashed) and the Z^0 decay width (2.5×10^{-6} GeV, brown dotted) in the $(\log_{10}\alpha', \log_{10} M_{Z'})$ plane. For the relic density, we show three contours with $\Omega h^2 = 0.106$ for $M_{\psi_D} = 10$ GeV, 100 GeV and 1000 GeV. The blue band is allowed by $\Delta a_\mu = (302 \pm 88) \times 10^{-11}$ within 3 σ.

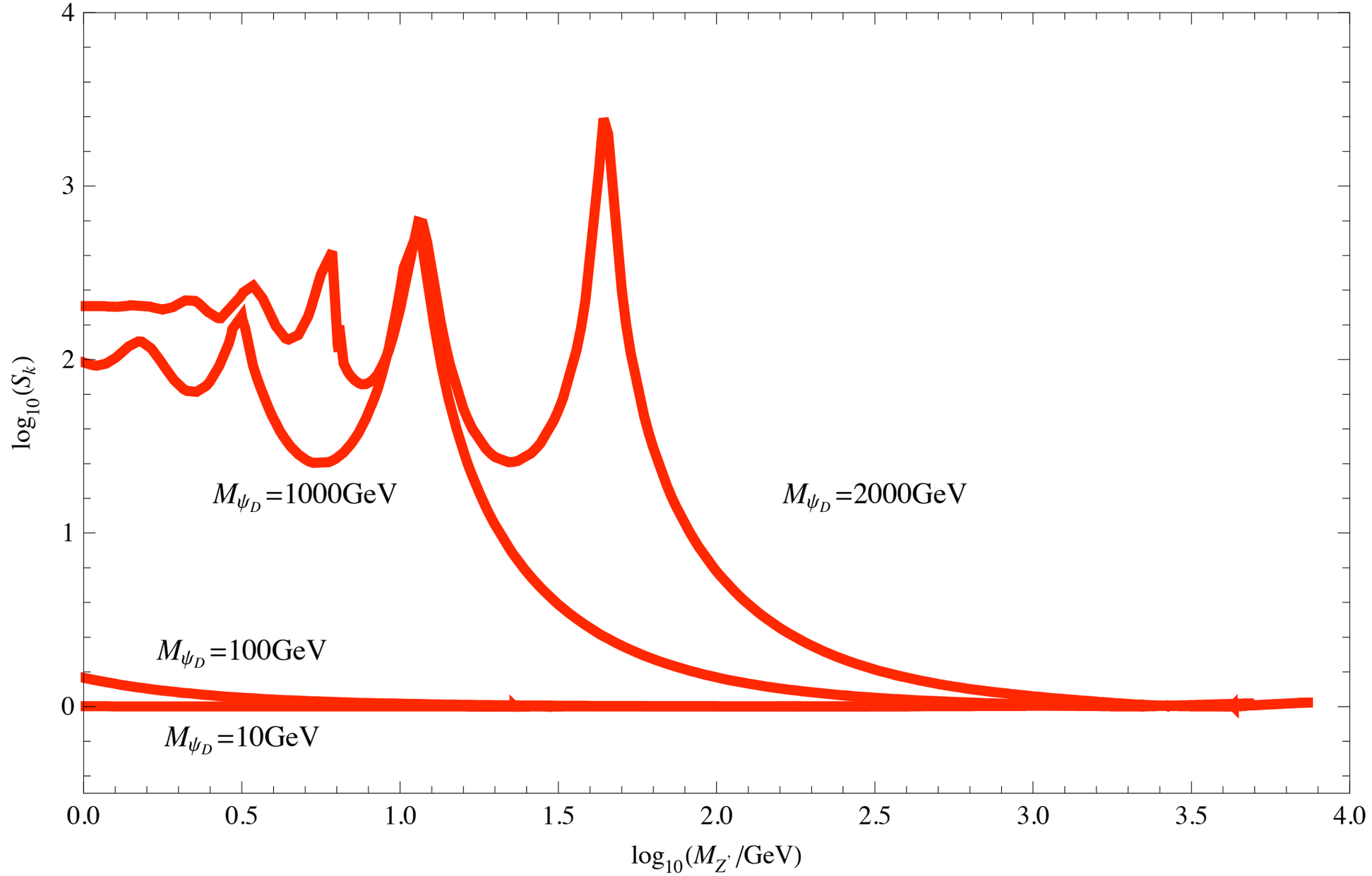

Figure: Sommerfeld enhancement factor along the constant relic density lines. $v = 200$ km/s.

$L_\mu - L_\tau$

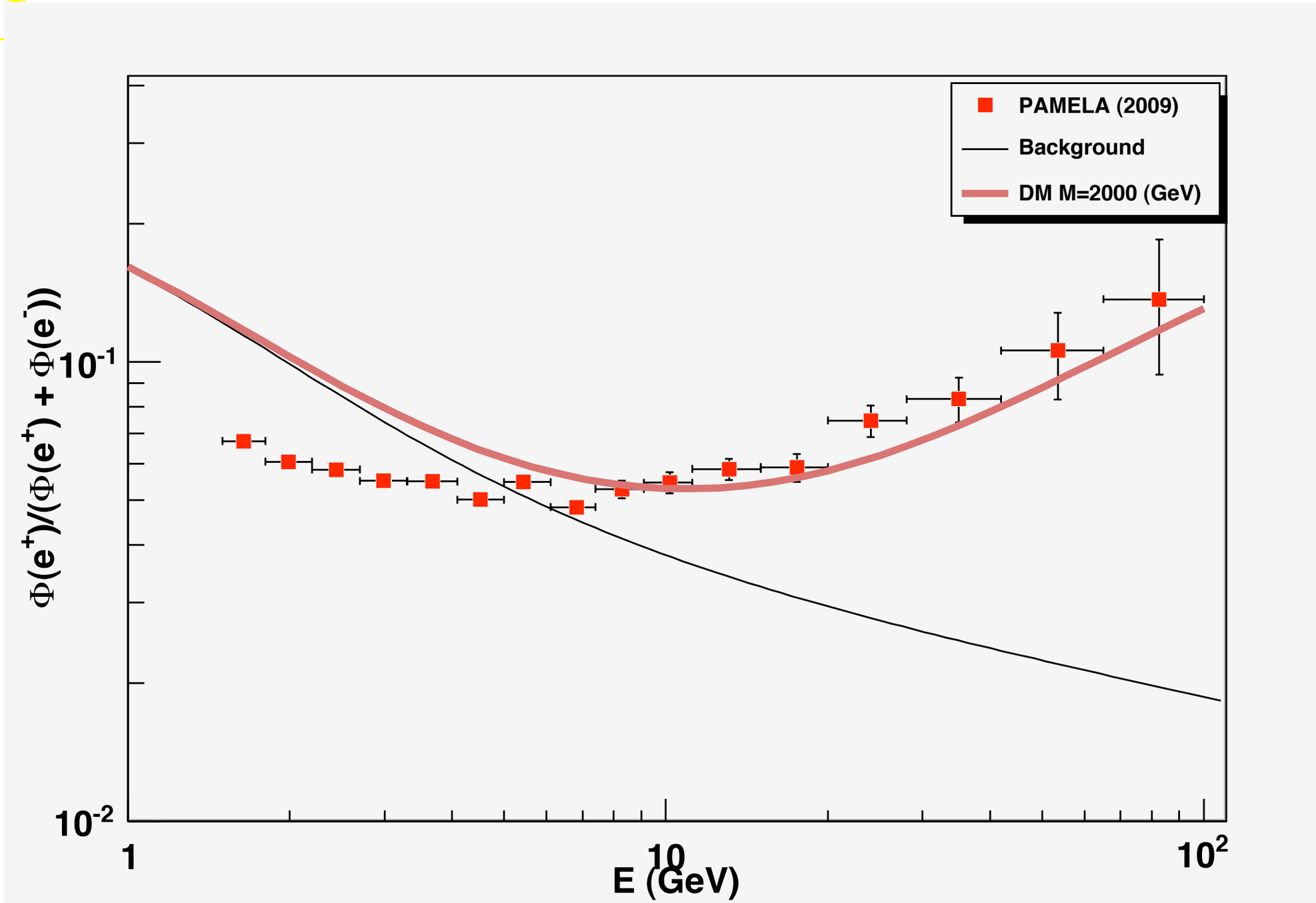

PAMELA positron ratio to (electro + positron)

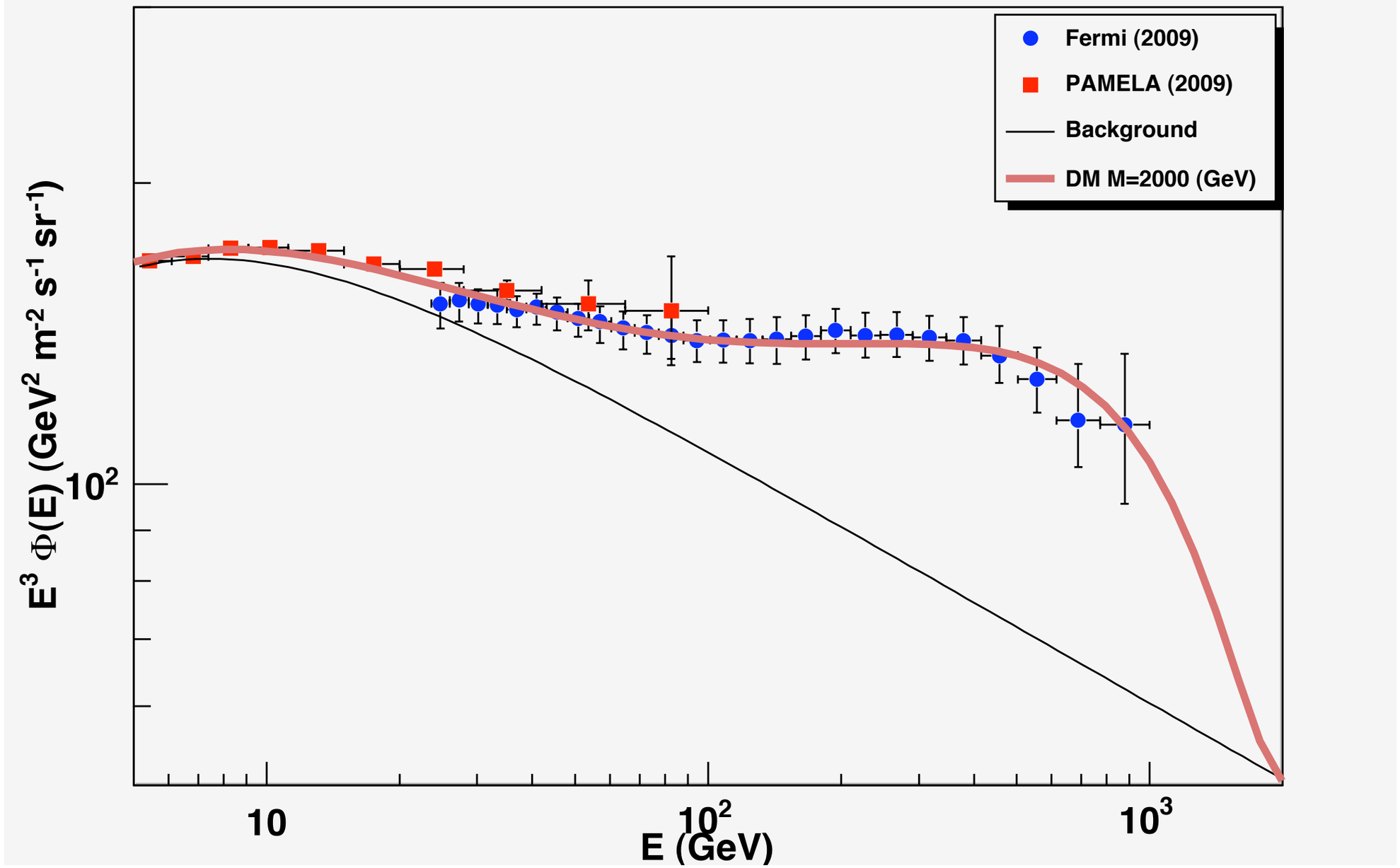

PAMELA + FERMI with bkgd x 0.67 and large boost factor ~O(5000)

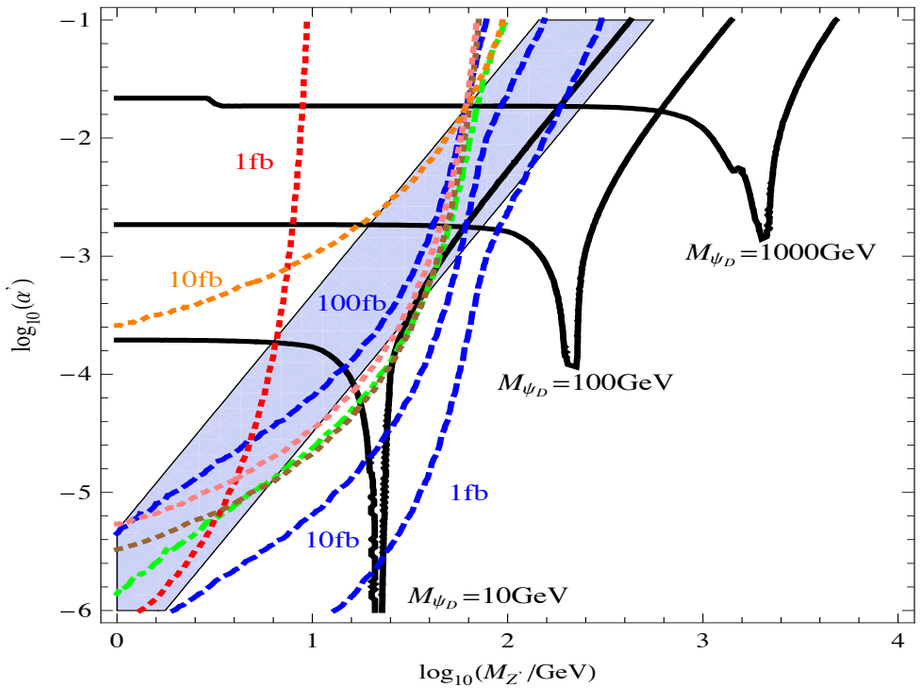

Figure 1: The relic density of CDM (black), the muon $(g-2)_\mu$ (blue band), the production cross section at B factories (1 fb, red dotted), Tevatron (10 fb, green dotdashed), LEP (10 fb, pink dotted), LEP2 (10 fb, orange dotted), LHC (1 fb, 10 fb, 100 fb, blue dashed) and the Z^0 decay width (2.5×10^{-6} GeV, brown dotted) in the $(\log_{10}\alpha', \log_{10} M_{Z'})$ plane. For the relic density, we show three contours with $\Omega h^2 = 0.106$ for $M_{\psi_D} = 10$ GeV, 100 GeV and 1000 GeV. The blue band is allowed by $\Delta a_\mu = (302 \pm 88) \times 10^{-11}$ within 3 σ.

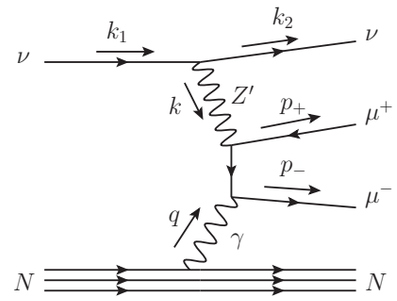

FIG. 1. The leading order contribution of the Z′ to neutrino trident production (another diagram with μ^+ and μ^- reversed i in g' ε

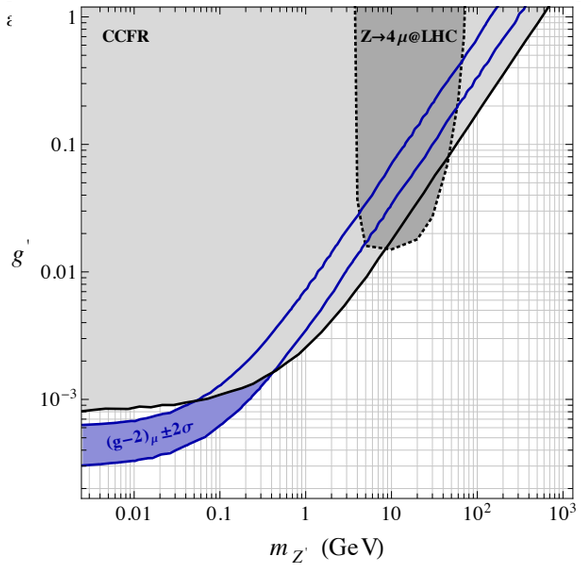

FIG. 2. Parameter space for the Z′ gauge boson. The light-grey area is excluded at 95% C.L. by the CCFR measurement of the neutrino trident cross-section. The grey region with the dotted contour is excluded by measurements of the SM

Seungwon Baek, Pyungwon Ko, arXiv:0811.1646, JCAP(2009) about PAMELA e^+ excess

Altmannshofer et al. arXiv:1406.2332 [hep-ph]

Neutrino trident puts strong constraints on this model

One can evade the neutrino trident constraint, if one introduces New fermions and generate muon g-2 at loop level w/ new fermions !

$U(1)_{L_\mu - L_\tau}$ -charged DM : Z' only vs. $Z' + \phi$

Z' Only

- Consider light Z' and $g_X \sim (\text{a few}) \times 10^{-4}$ for the muon g-2. Then
- $\chi\bar{\chi} \to Z'^{*} \to f_{\rm SM}\bar{f}_{\rm SM}$: dominant annihilation channel
- $g_X \sim 10^{-4}$ is too small for $\chi\bar{\chi} \to Z'Z'$ to be effective for $\Omega_\chi h^2$
- $m_{Z'} \sim 2m_{\rm DM}$ with the s-channel Z' resonance for the correct relic density
- Many recent studies on this case:

  - Asai, Okawa, Tsumura, 2011.03165
  - Holst, Hooper, Krnjaic, 2107.09067
  - Drees and Zhao, arXiv:2107.14528
  - And some earlier papers

However DM with massive dark photon can not be complete without Dark Higgs !

This is the main message of this talk !

cf: Let me call Z' , $U(1)_{L_\mu - L_\tau}$ gauge boson, "dark photon", since it couples to DM

Digression on the role of Dark Higgs

Higgs portal DM models

$$\mathcal{L}_{\rm scalar} = \frac{1}{2}\partial_\mu S \partial^\mu S - \frac{1}{2}m_S^2 S^2 - \frac{\lambda_{HS}}{2} H^\dagger H S^2 - \frac{\lambda_S}{4} S^4$$

$$\mathcal{L}_{\rm fermion} = \overline{\psi}\left[i\gamma\cdot\partial - m_\psi\right]\psi - \frac{\lambda_{H\psi}}{\Lambda} H^\dagger H\ \overline{\psi}\psi$$

$$\mathcal{L}_{\rm vector} = -\frac{1}{4}V_{\mu\nu}V^{\mu\nu} + \frac{1}{2}m_V^2 V_\mu V^\mu + \frac{1}{4}\lambda_V (V_\mu V^\mu)^2 + \frac{1}{2}\lambda_{HV} H^\dagger H V_\mu V^\mu.$$

All invariant under ad hoc Z2 symmetry

arXiv:1112.3299, … 1402.6287, etc.

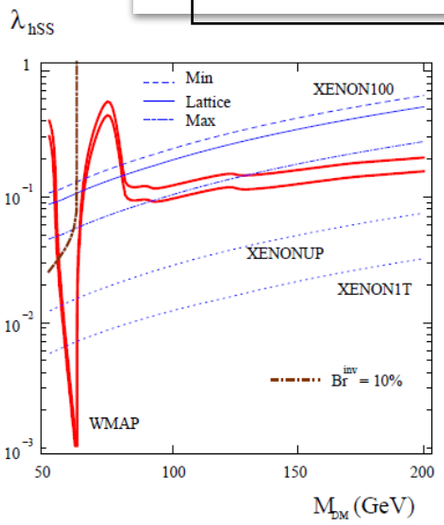

FIG. 1. Scalar Higgs-portal parameter space allowed by WMAP (between the solid red curves), XENON100 and $\mathrm{BR}^{\rm inv} = 10\%$ for $m_h = 125$ GeV. Shown also are the prospects for XENON upgrades.

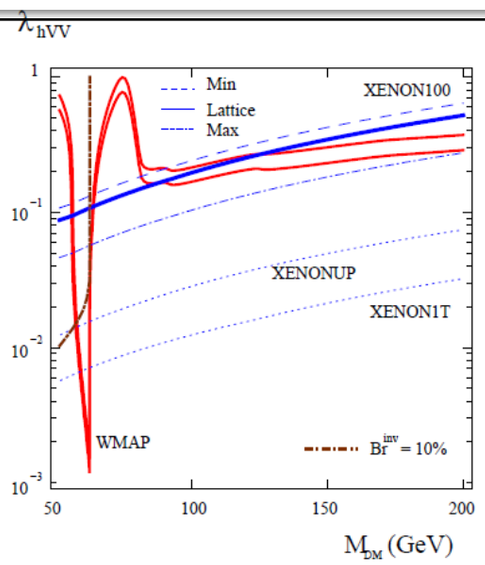

FIG. 2. Same as Fig. 1 for vector DM particles.

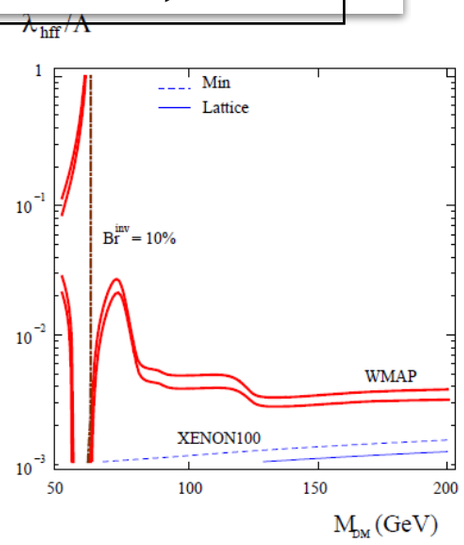

FIG. 3. Same as in Fig.1 for fermion DM; λ_{hff}/Λ is in GeV^{-1}.

Higgs portal DM as examples

$$\mathcal{L}_{\rm scalar} = \frac{1}{2}\partial_\mu S \partial^\mu S - \frac{1}{2}m_S^2 S^2 - \frac{\lambda_{HS}}{2} H^\dagger H S^2 - \frac{\lambda_S}{4} S^4$$

$$\mathcal{L}_{\rm fermion} = \overline{\psi}\left[i\gamma\cdot\partial - m_\psi\right]\psi - \frac{\lambda_{H\psi}}{\Lambda} H^\dagger H\ \overline{\psi}\psi$$

$$\mathcal{L}_{\rm vector} = -\frac{1}{4}V_{\mu\nu}V^{\mu\nu} + \frac{1}{2}m_V^2 V_\mu V^\mu + \frac{1}{4}\lambda_V (V_\mu V^\mu)^2 + \frac{1}{2}\lambda_{HV} H^\dagger H V_\mu V^\mu .$$

All invariant under ad hoc Z2 symmetry

arXiv:1112.3299, … 1402.6287, etc.

We need to include dark Higgs or singlet scalar to get renormalizable/unitary models for Higgs portal singlet fermion or vector DM

[NB: UV Completions : Not unique]

$m_h = 125$ GeV. Shown also are the prospects for XENON upgrades.

FIG. 2. Same as Fig. 1 for vector DM particles.

FIG. 3. Same as in Fig.1 for fermion DM; λ_{hff}/Λ is in GeV^{-1}.

Models for HP SFDM & VDM

UV Completion of HP Singlet Fermion DM (SFDM)

$$
\begin{aligned}
\mathcal{L} &= \mathcal{L}_{\rm SM} - \mu_{HS} S H^\dagger H - \frac{\lambda_{HS}}{2} S^2 H^\dagger H \\
&\quad + \frac{1}{2}(\partial_\mu S \partial^\mu S - m_S^2 S^2) - \mu_S^3 S - \frac{\mu'_S}{3} S^3 - \frac{\lambda_S}{4} S^4 \\
&\quad + \overline{\psi}(i \not{\partial} - m_{\psi_0})\psi - \lambda S \overline{\psi}\psi
\end{aligned}
$$

UV Completion of HP VDM

$$
\begin{aligned}
\mathcal{L}_{VDM} = & -\frac{1}{4} X_{\mu\nu} X^{\mu\nu} + (D_\mu \Phi)^\dagger (D^\mu \Phi) - \frac{\lambda_\Phi}{4} \left(\Phi^\dagger \Phi - \frac{v_\Phi^2}{2} \right)^2 \\
& - \lambda_{H\Phi} \left(H^\dagger H - \frac{v_H^2}{2} \right) \left(\Phi^\dagger \Phi - \frac{v_\Phi^2}{2} \right) \ ,
\end{aligned}
$$

- **The simplest UV completions in terms of # of new d.o.f.**
- **At least, 2 more parameters, (m_ϕ , $\sin\alpha$) for DM physics**

UV Completion for HP FDM

Baek, Ko, Park, arXiv:1112.1847

$$\begin{aligned}\mathcal{L} &= \mathcal{L}_{\rm SM} - \mu_{HS} S H^\dagger H - \frac{\lambda_{HS}}{2} S^2 H^\dagger H \\ &+ \frac{1}{2}(\partial_\mu S \partial^\mu S - m_S^2 S^2) - \mu_S^3 S - \frac{\mu'_S}{3} S^3 - \frac{\lambda_S}{4} S^4 \\ &+ \overline{\psi}(i \not{\partial} - m_{\psi_0})\psi - \lambda S \overline{\psi}\psi\end{aligned}$$

mixing

invisible decay

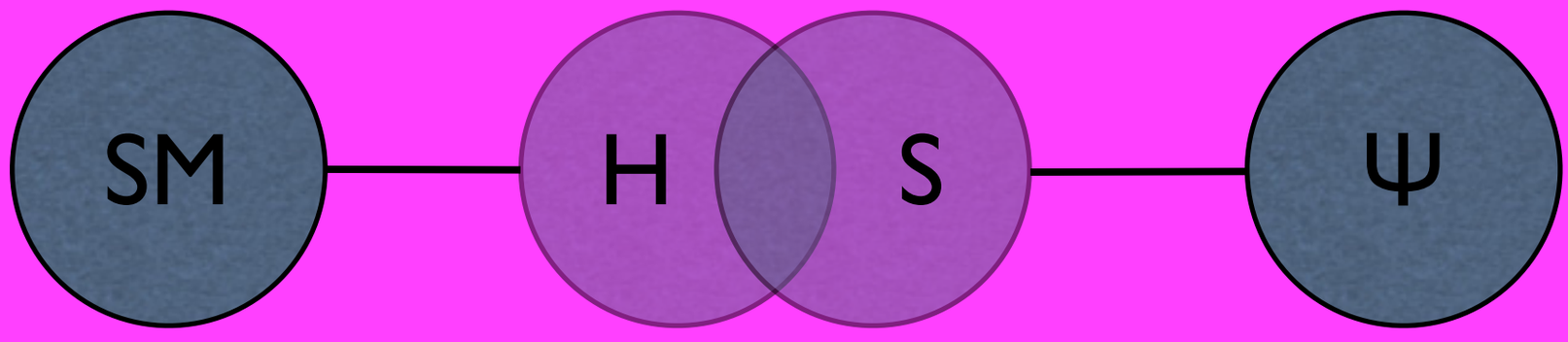

Production and decay rates are suppressed relative to SM.

Higgs-Singlet Mixing

- Mixing and Eigenstates of Higgs-like bosons

$$\mu_H^2 = \lambda_H v_H^2 + \mu_{HS} v_S + \frac{1}{2}\lambda_{HS} v_S^2,$$

$$m_S^2 = -\frac{\mu_S^3}{v_S} - \mu_S' v_S - \lambda_S v_S^2 - \frac{\mu_{HS} v_H^2}{2 v_S} - \frac{1}{2}\lambda_{HS} v_H^2,$$

at vacuum

$$M^2_{\text{Higgs}} \equiv \begin{pmatrix} m^2_{hh} & m^2_{hs} \\ m^2_{hs} & m^2_{ss} \end{pmatrix} \equiv \begin{pmatrix} \cos\alpha & \sin\alpha \\ -\sin\alpha & \cos\alpha \end{pmatrix} \begin{pmatrix} m_1^2 & 0 \\ 0 & m_2^2 \end{pmatrix} \begin{pmatrix} \cos\alpha & -\sin\alpha \\ \sin\alpha & \cos\alpha \end{pmatrix}$$

$$H_1 = h\cos\alpha - s\sin\alpha,$$
$$H_2 = h\sin\alpha + s\cos\alpha.$$

Mixing of Higgs and singlet

Constraints

- Dark matter to nucleon cross section (constraint)

$$\sigma_p \approx \frac{1}{\pi}\mu^2\lambda_p^2 \simeq 2.7\times 10^{-2}\frac{m_p^2}{\pi}\left|\left(\frac{m_p}{v}\right)\lambda \sin\alpha\cos\alpha\left(\frac{1}{m_1^2}-\frac{1}{m_2^2}\right)\right|^2$$

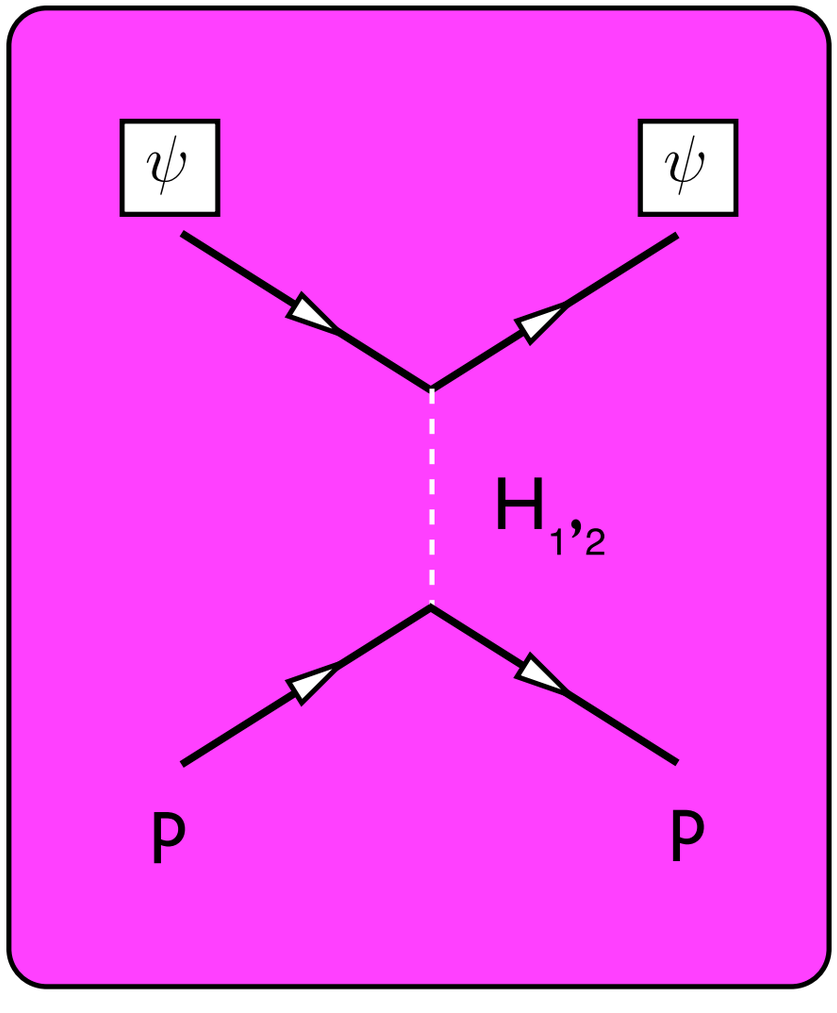

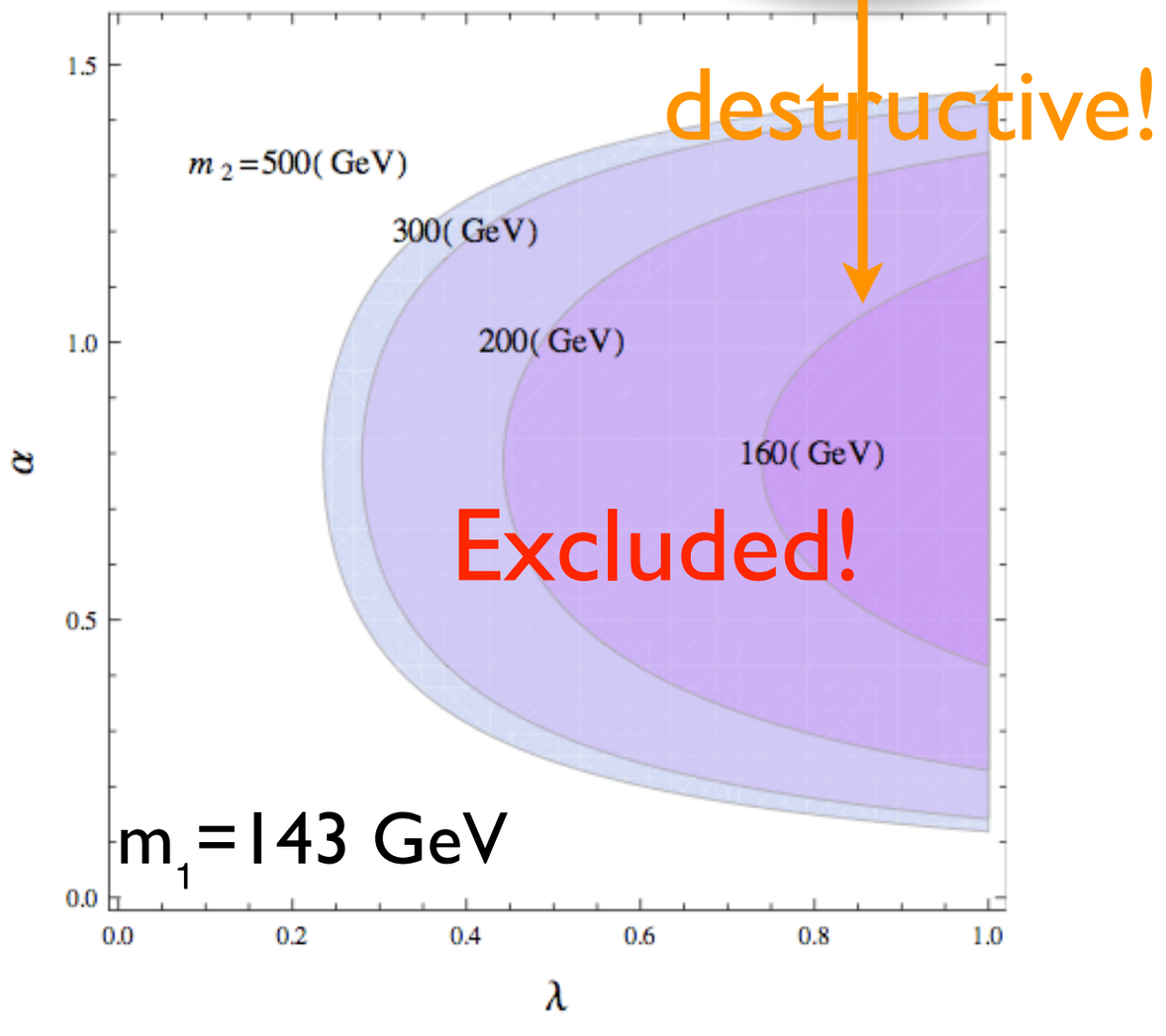

Low energy pheno.

- Universal suppression of collider SM signals

[See 1112.1847, Seungwon Baek, P. Ko & WIP]

- If "$m_h > 2\, m_\phi$", non-SM Higgs decay!

- Tree-level shift of $\lambda_{H,SM}$ (& loop correction)

$$\lambda_{\Phi H} \Rightarrow \lambda_H = \left[1 + \left(\frac{m_\phi^2}{m_h^2} - 1\right) \sin^2\alpha\right] \lambda_H^{\rm SM}$$

⇨ If "$m_\phi > m_h$", vacuum instability can be cured.

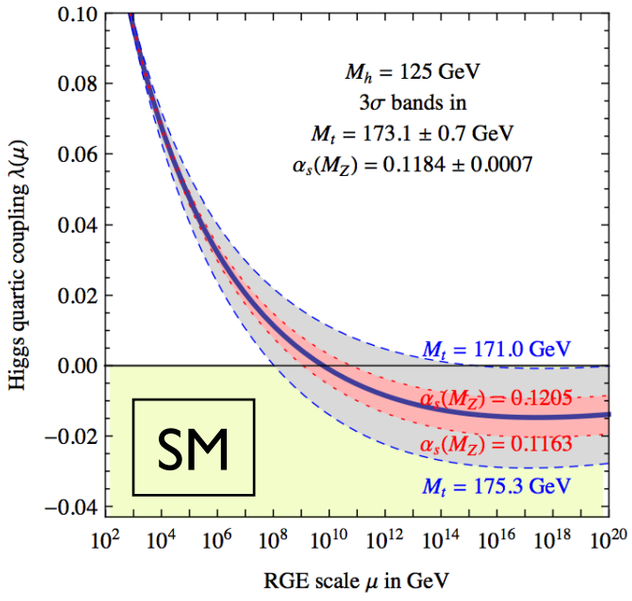

[G. Degrassi et al., 1205.6497]

α

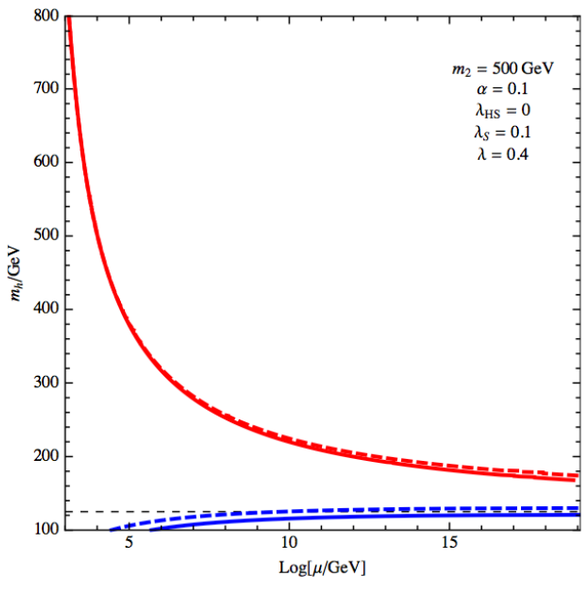

[S. Baek, P. Ko, WIP & E. Senaha, JHEP(2012)]

UV Completion of HP VDM

[S Baek, P Ko, WI Park, E Senaha, arXiv:1212.2131 (JHEP)]

$$\mathcal{L}_{VDM} = -\frac{1}{4}X_{\mu\nu}X^{\mu\nu} + (D_\mu\Phi)^\dagger(D^\mu\Phi) - \frac{\lambda_\Phi}{4}\left(\Phi^\dagger\Phi - \frac{v_\Phi^2}{2}\right)^2$$
$$-\lambda_{H\Phi}\left(H^\dagger H - \frac{v_H^2}{2}\right)\left(\Phi^\dagger\Phi - \frac{v_\Phi^2}{2}\right) \ ,$$

$X_\mu \equiv V_\mu$ here

$$\boxed{\Phi(x) = (v_\phi + \phi(x))/\sqrt{2}}$$

- There appear a new singlet scalar (dark Higgs) $\phi(x)$ from $\Phi(x)$, which mixes with the SM Higgs boson through Higgs portal interaction ($\lambda_{H\Phi}$ term)
- The effects must be similar to the singlet scalar in the fermion CDM model, and generically true in the DM with dark gauge symmetry
- Can accommodate GeV scale gamma ray excess from GC with $VV \to \phi\phi$
- **Can modify the Higgs inflation : No tight correlation with top mass**

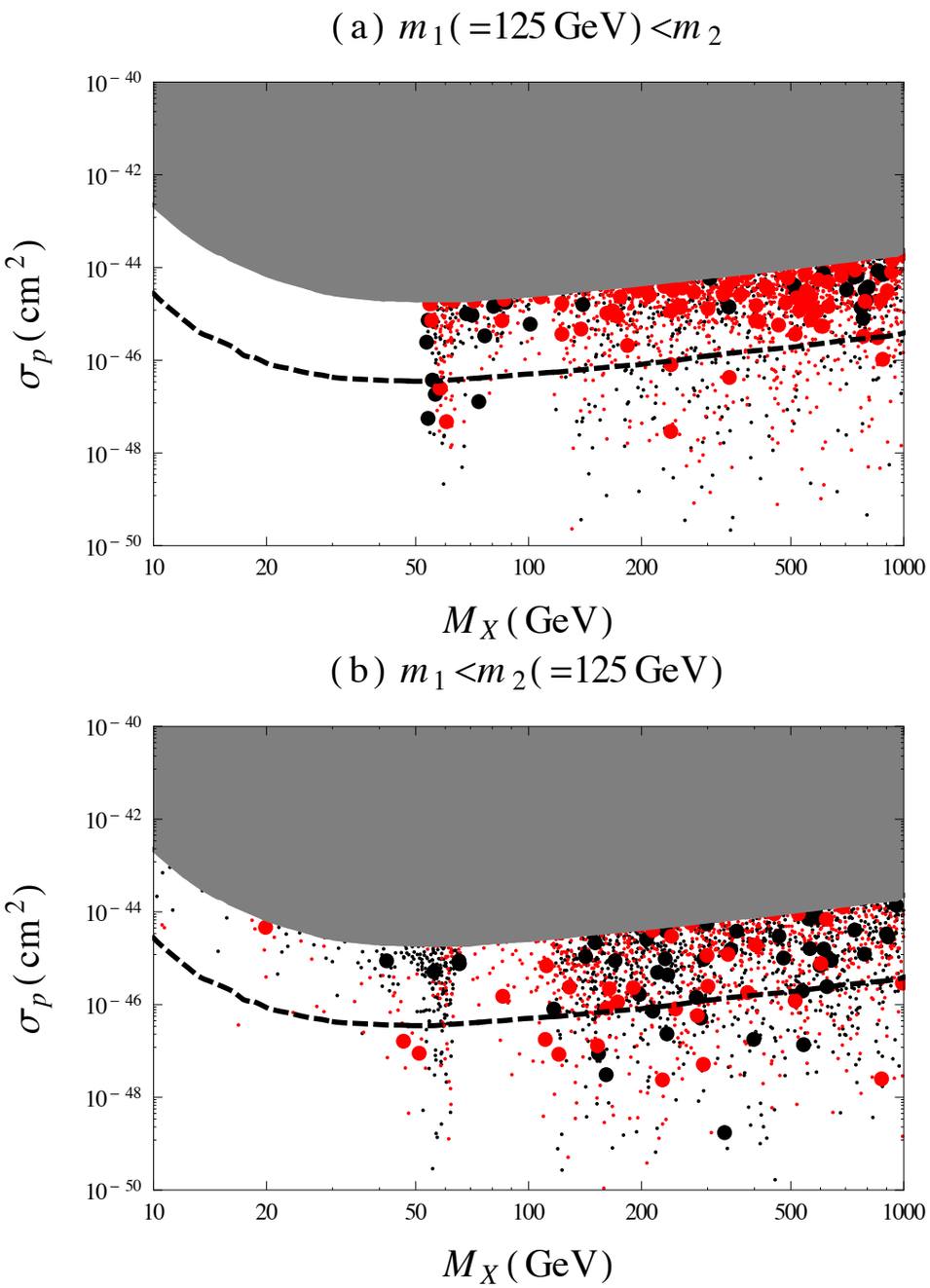

Figure 6. The scattered plot of σ_p as a function of M_X. The big (small) points (do not) satisfy the WMAP relic density constraint within 3 σ, while the red-(black-)colored points gives $r_1 > 0.7 (r_1 < 0.7)$. The grey region is excluded by the XENON100 experiment. The dashed line denotes the sensitivity of the next XENON experiment, XENON1T.

New scalar (Dark Higgs) improves EW vacuum stability

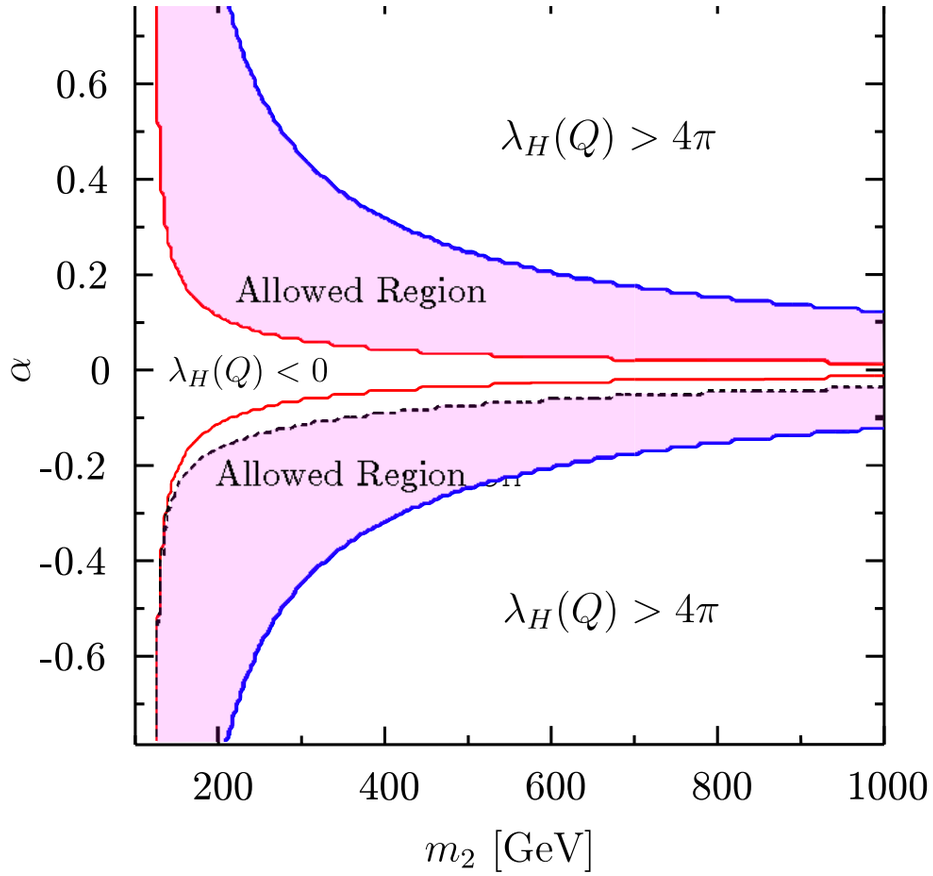

Figure 8. The vacuum stability and perturbativity constraints in the α-m_2 plane. We take $m_1 = 125$ GeV, $g_X = 0.05$, $M_X = m_2/2$ and $v_\Phi = M_X/(g_X Q_\Phi)$.

Interaction Lagrangians

Scalar DM

$$\mathcal{L}^{\rm int}_{\rm SDM} = -h\,\left(\frac{2m_W^2}{v_h}W_\mu^+W^{-\mu} + \frac{m_Z^2}{v_h}Z_\mu Z^\mu\right) - \lambda_{HS}v_h\;hS^2.$$

Singlet FDM

$$\mathcal{L}^{\rm int}_{\rm FDM} = -\left(H_1\cos\alpha + H_2\sin\alpha\right)\left(\sum_f \frac{m_f}{v_h}\bar{f}f - \frac{2m_W^2}{v_h}W_\mu^+W^{-\mu} - \frac{m_Z^2}{v_h}Z_\mu Z^\mu\right)$$
$$+\,g_\chi\left(H_1\sin\alpha - H_2\cos\alpha\right)\;\bar{\chi}\chi\;.$$

Vector DM

$$\mathcal{L}^{\rm int}_{\rm VDM} = -\left(H_1\cos\alpha + H_2\sin\alpha\right)\left(\sum_f \frac{m_f}{v_h}\bar{f}f - \frac{2m_W^2}{v_h}W_\mu^+W^{-\mu} - \frac{m_Z^2}{v_h}Z_\mu Z^\mu\right)$$
$$-\,\frac{1}{2}g_V m_V\left(H_1\sin\alpha - H_2\cos\alpha\right)\;V_\mu V^\mu\;.$$

NB: One can not ignore 125 GeV Higgs Boson or singlet scalar by hand : Not Well defined EFT, Breaks gauge invariance, etc.

Collider Implications

$m_h = 125\text{GeV},\ \text{Br}(H \to \text{inv}) < 0.51$ at 90% CL

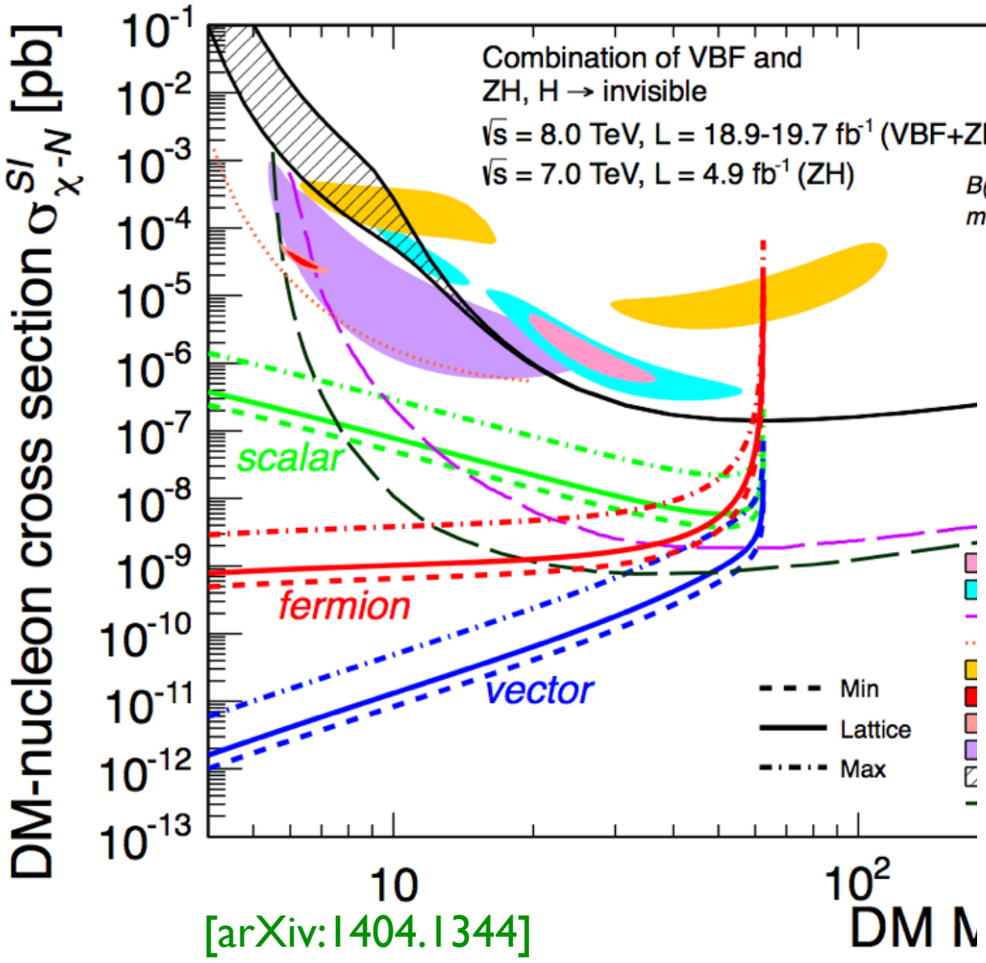

[arXiv:1404.1344]

Based on EFTs

$m_h = 125.5\text{GeV},\ \text{Br}(H \to \text{inv}) < 0.52$ at 90% CL

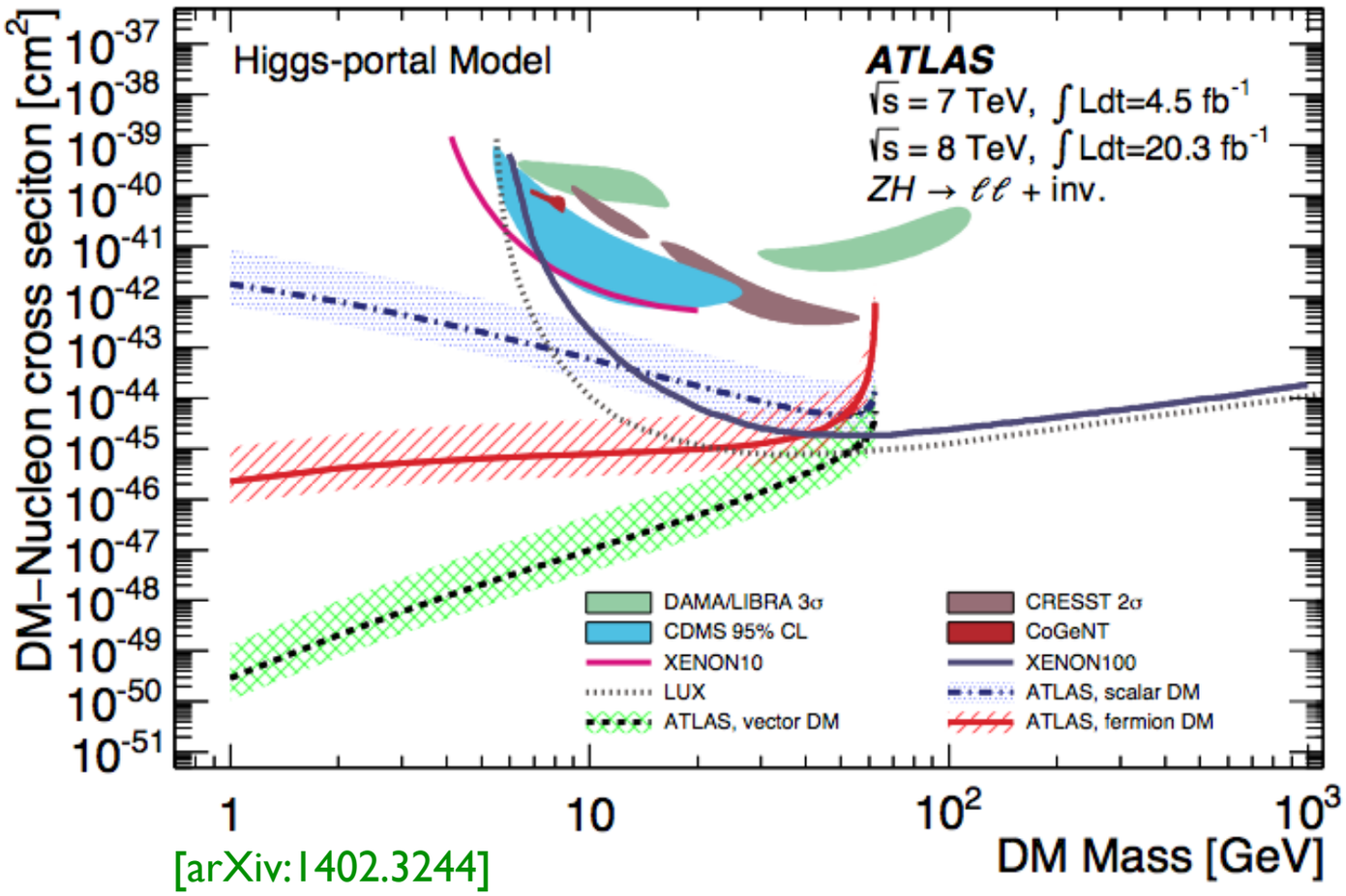

[arXiv:1402.3244]

- However, in renormalizable unitary models of Higgs portals, 2 more relevant parameters !

$$\mathcal{L}_{\rm SFDM} = \overline{\psi}\left(i\partial - m_\psi - \lambda_\psi S\right) - \mu_{HS} S H^\dagger H - \frac{\lambda_{HS}}{2} S^2 H^\dagger H$$
$$+ \frac{1}{2}\partial_\mu S \partial^\mu S - \frac{1}{2} m_S^2 S^2 - \mu_S^3 S - \frac{\mu_S^{'}}{3} S^3 - \frac{\lambda_S}{4} S^4.$$

[arXiv: 1405.3530, S. Baek, P. Ko & WIPark, PRD]

$$\mathcal{L}_{\rm VDM} = -\frac{1}{4} V_{\mu\nu} V^{\mu\nu} + D_\mu \Phi^\dagger D^\mu \Phi - \lambda_\Phi \left(\Phi^\dagger\Phi - \frac{v_\Phi^2}{2}\right)^2 - \lambda_{\Phi H}\left(\Phi^\dagger\Phi - \frac{v_\Phi^2}{2}\right)\left(H^\dagger H - \frac{v_H^2}{2}\right)$$

$$\sigma_p^{\rm SI} = (\sigma_p^{\rm SI})_{\rm EFT}\, c_\alpha^4 m_h^4 \mathcal{F}(m_{\rm DM}, \{m_i\}, v)$$
$$\simeq (\sigma_p^{\rm SI})_{\rm EFT}\, c_\alpha^4 \left(1 - \frac{m_h^2}{m_2^2}\right)^2$$

Dashed curves:EFT, ATLAS,CMS results

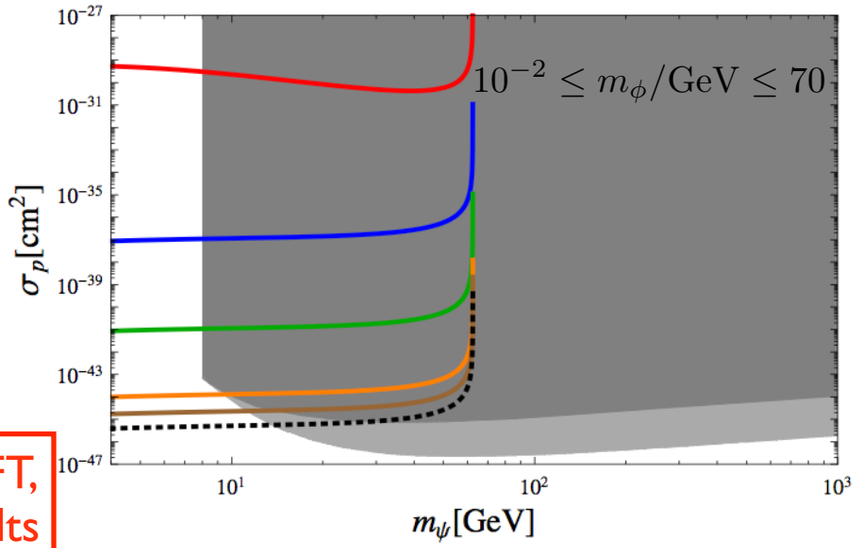

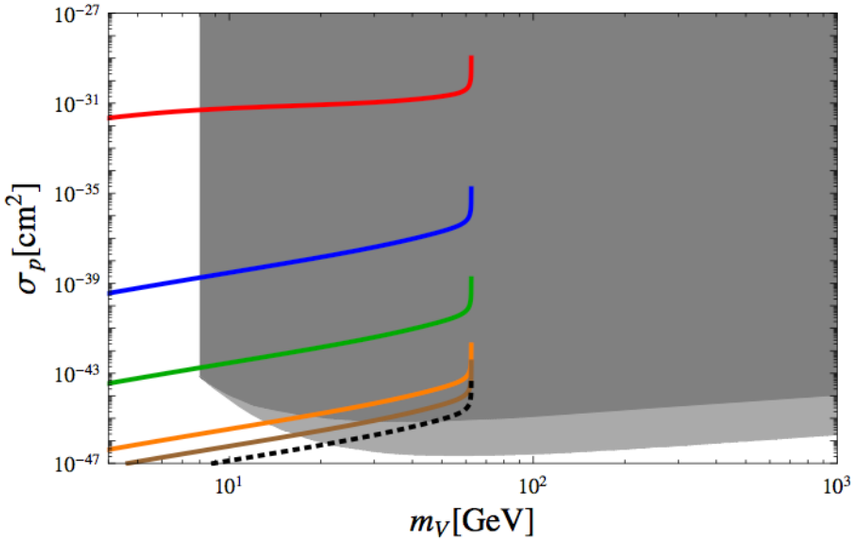

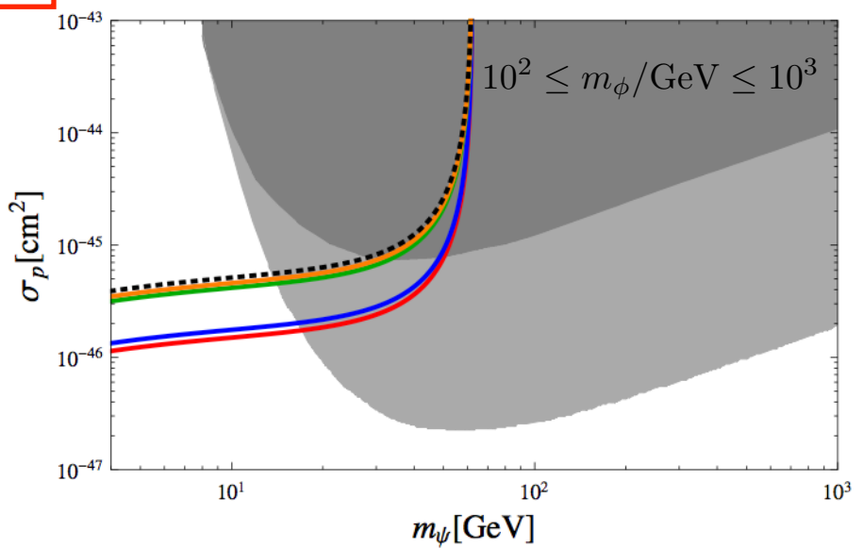

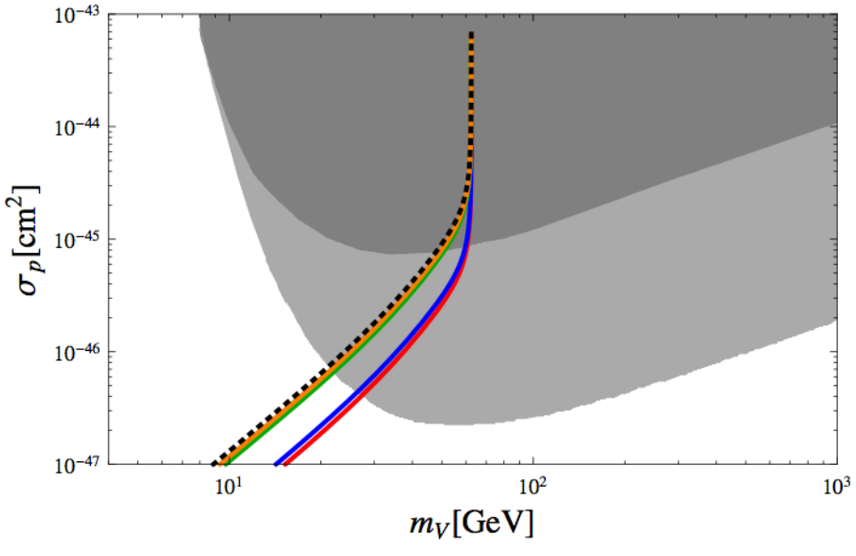

- However, in renormalizable unitary models of Higgs portals, 2 more relevant parameters

$$\mathcal{L}_{\rm SFDM} = \overline{\psi}\left(i\partial - m_\psi - \lambda_\psi S\right) - \mu_{HS} S H^\dagger H - \frac{\lambda_{HS}}{2} S^2 H^\dagger H$$
$$+ \frac{1}{2}\partial_\mu S \partial^\mu S - \frac{1}{2} m_S^2 S^2 - \mu_S^3 S - \frac{\mu_S^{'}}{3} S^3 - \frac{\lambda_S}{4} S^4.$$

[arXiv: 1405.3530, S. Baek, P. Ko & WIPark, PRD]

$$\sigma_p^{\rm SI} = (\sigma_p^{\rm SI})_{\rm EFT}\; c_\alpha^4 m_h^4 \mathcal{F}(m_{\rm DM}, \{m_i\}, v)$$
$$\simeq (\sigma_p^{\rm SI})_{\rm EFT}\; c_\alpha^4 \left(1 - \frac{m_h^2}{m_2^2}\right)^2$$

$$\mathcal{L}_{\rm VDM} = -\frac{1}{4} V_{\mu\nu} V^{\mu\nu} + D_\mu \Phi^\dagger D^\mu \Phi - \lambda_\Phi \left(\Phi^\dagger\Phi - \frac{v_\Phi^2}{2}\right)^2 - \lambda_{\Phi H}\left(\Phi^\dagger\Phi - \frac{v_\Phi^2}{2}\right)\left(H^\dagger H - \frac{v_H^2}{2}\right)$$

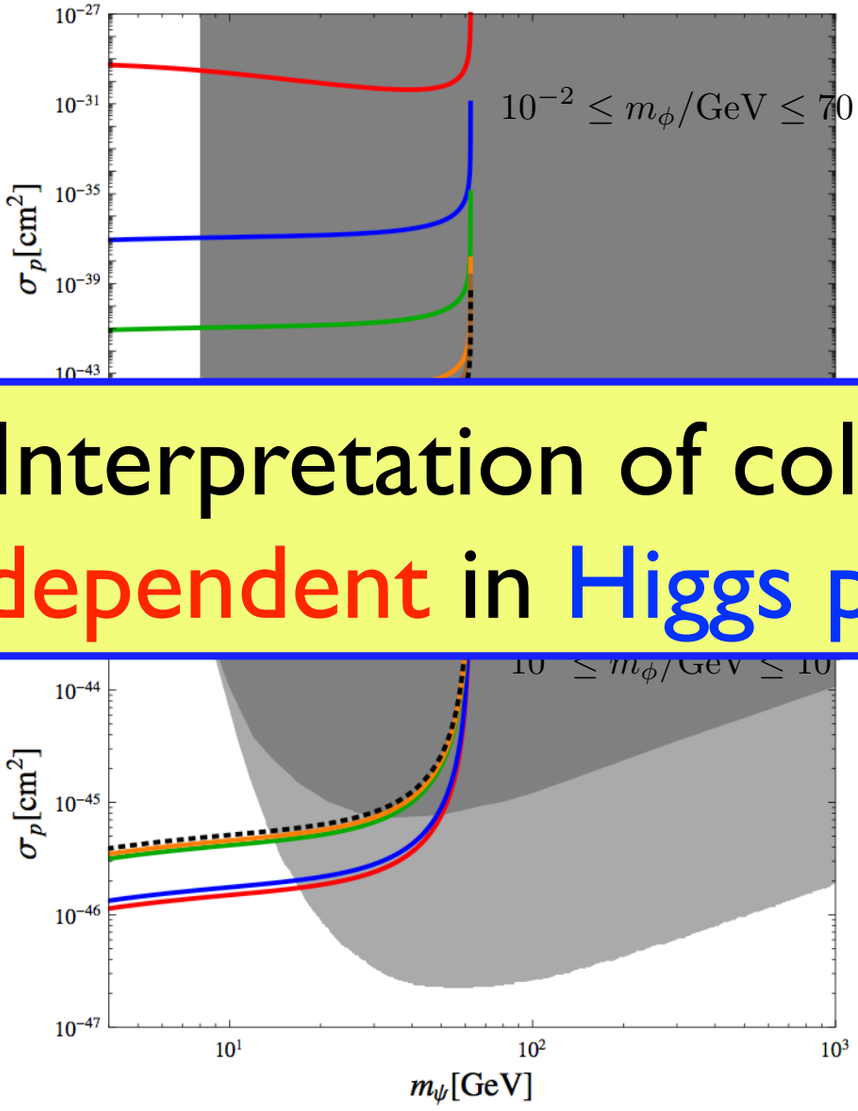

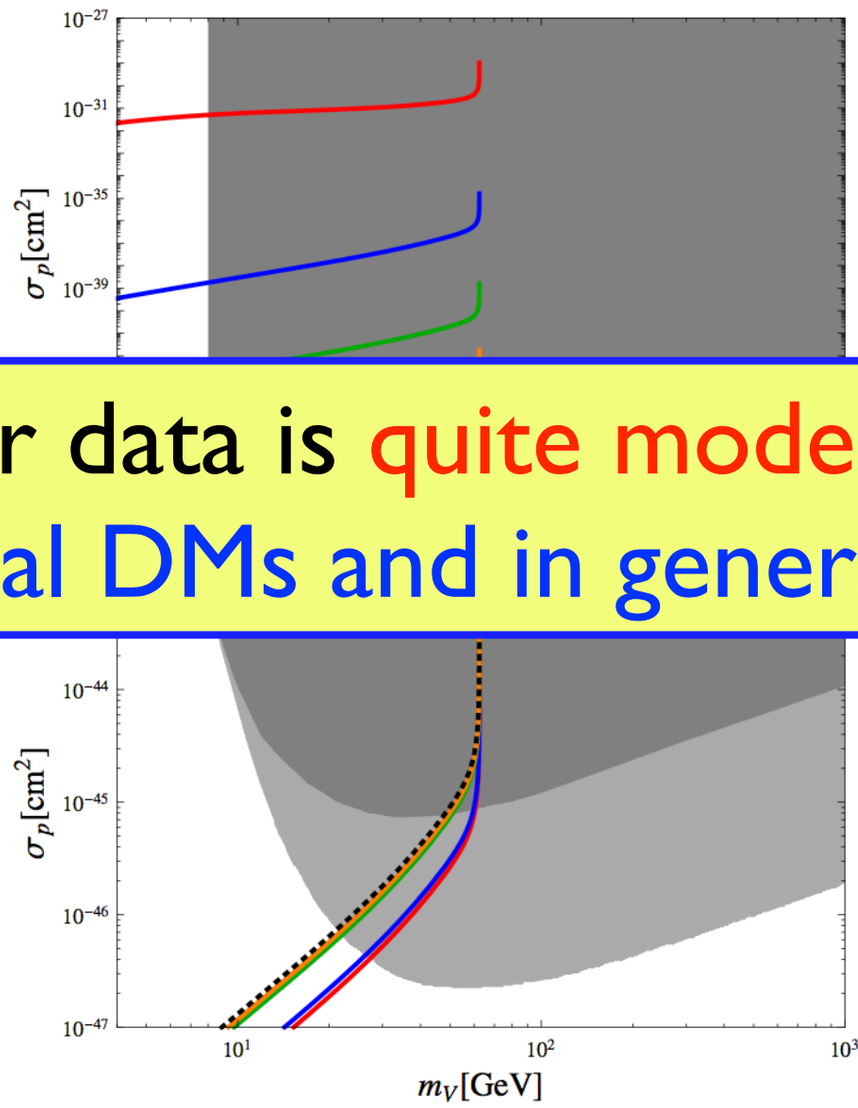

Interpretation of collider data is quite model-dependent in Higgs portal DMs and in general

Invisible H decay into a pair of VDM

[arXiv: 1405.3530, S. Baek, P. Ko & WI Park, PRD]

$$(\Gamma_h^{\rm inv})_{\rm EFT} = \frac{\lambda_{VH}^2}{128\pi}\frac{v_H^2 m_h^3}{m_V^4} \times \left(1-\frac{4m_V^2}{m_h^2}+12\frac{m_V^4}{m_h^4}\right)\left(1-\frac{4m_V^2}{m_h^2}\right)^{1/2} \quad (23)$$

VS.

$$\Gamma_i^{\rm inv} = \frac{g_X^2}{32\pi}\frac{m_i^3}{m_V^2}\left(1-\frac{4m_V^2}{m_i^2}+12\frac{m_V^4}{m_i^4}\right)\left(1-\frac{4m_V^2}{m_i^2}\right)^{1/2}\sin^2\alpha \quad (22)$$

Invisible H decay width : finite for small mV in unitary/renormalizable model

Two Limits for $m_V \to 0$

Also see the addendum (under review now) by S Baek, P Ko, WI Park

- $m_V = g_X Q_\Phi v_\Phi$ in the UV completion with dark Higgs boson

- Case I : $g_X \to 0$ with finite $v_\Phi \neq 0$

$$\frac{g_X^2 Q_\Phi^2}{m_V^2} = \frac{g_X^2 Q_\Phi^2}{g_X^2 Q_\Phi^2 v_\Phi^2} = \frac{1}{v_\Phi^2} = \text{finite.}$$

$$\left(\Gamma_h^{\text{inv}}\right)_{\text{UV}} = \frac{1}{32\pi}\frac{m_h^3}{v_\Phi^2}\sin^2\alpha = \Gamma(h \to a_\Phi a_\Phi)$$

with a_Φ being the NG boson for spontaneously broken global $U(1)_X$

- Case II : $v_\Phi \to 0$ with finite $g_X \neq 0$

$$\alpha \xrightarrow{v_\Phi \to 0^+} \frac{2\lambda_{H\Phi} v_\Phi}{\lambda_H v_H}$$

$$\frac{g_X^2 Q_\Phi^2}{m_V^2}\sin^2\alpha \xrightarrow{v_\Phi \to 0^+} \frac{4\lambda_{H\Phi}^2}{\lambda_H^2 v_H^2} = \frac{2\lambda_{H\Phi}^2}{\lambda_H m_h^2} = \text{finite,}$$

$$\left(\Gamma_h^{\text{inv}}\right)_{\text{UV}} \xrightarrow{v_\Phi \to 0^+} \frac{1}{16\pi}\frac{\lambda_{H\Phi}^2 m_h}{\lambda_H}$$

Therefore $\Gamma(h \to VV)$ is finite when $m_V \to 0$ in the UV completions

S. Baek, P. Ko, M. Park, WIPark, C.Yu,
arXiv:1506.06556, PLB (2016)

- EFT : Effective operator $\mathcal{L}_{int} = \frac{m_q}{\Lambda_{dd}^3}\bar{q}q\bar{\chi}\chi$
- S.M.: Simple scalar mediator S of
  $\mathcal{L}_{int} = \left(\frac{m_q}{v_H}\sin\alpha\right) S\bar{q}q - \lambda_s \cos\alpha S\bar{\chi}\chi$
- H.M.: A case where a Higgs is a mediator
  $\mathcal{L}_{int} = -\left(\frac{m_q}{v_H}\cos\alpha\right) H\bar{q}q - \lambda_s \sin\alpha H\bar{\chi}\chi$
- H.P.: Higgs portal model as in eq. (2).

$$\frac{d\sigma_i}{dm_{\chi\chi}} \propto \left|\frac{\sin 2\alpha\ g_\chi}{m_{\chi\chi}^2 - m_{H_1}^2 + i m_{H_1}\Gamma_{H_1}} - \frac{\sin 2\alpha\ g_\chi}{m_{\chi\chi}^2 - m_{H_2}^2 + i m_{H_2}\Gamma_{H_2}}\right|^2$$

$$\text{H.P.} \underset{m_{H_2}^2 \gg \hat{s}}{\longrightarrow} \text{H.M.},$$

$$\text{S.M.} \underset{m_S^2 \gg \hat{s}}{\longrightarrow} \text{EFT},$$

$$\text{H.M.} \neq \text{EFT}\,.$$

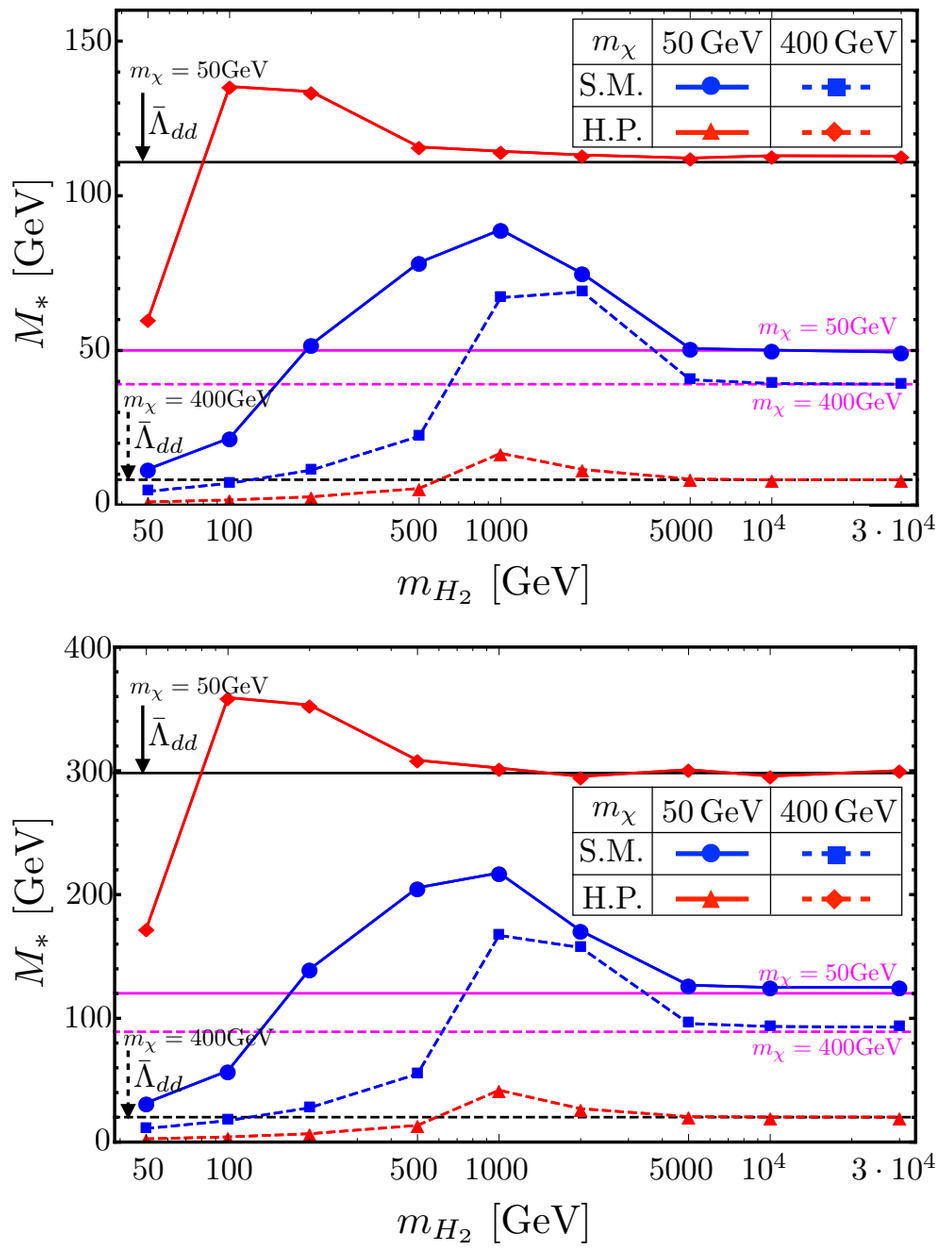

FIG. 3: The experimental bounds on M_* at 90% C.L. as a function of m_{H_2} (m_S in S.M. case) in the monojet+$\not{E}_T$ search (upper) and $t\bar{t} + \not{E}_T$ search (lower). Each line corresponds to the EFT approach (magenta), S.M. (blue), H.M. (black), and H.P. (red), respectively. The bound of S.M., H.M., and H.P., are expressed in terms of the effective mass M_* through the Eq.(16)-(20). The solid and dashed lines correspond to $m_\chi = 50$ GeV and 400 GeV in each model, respectively.

Fermi-LAT GC γ-ray

see arXiv:1612.05687 for a recent overview by
C.Karwin, S. Murgia, T. Tait, T.A.Porter, P. Tanedo

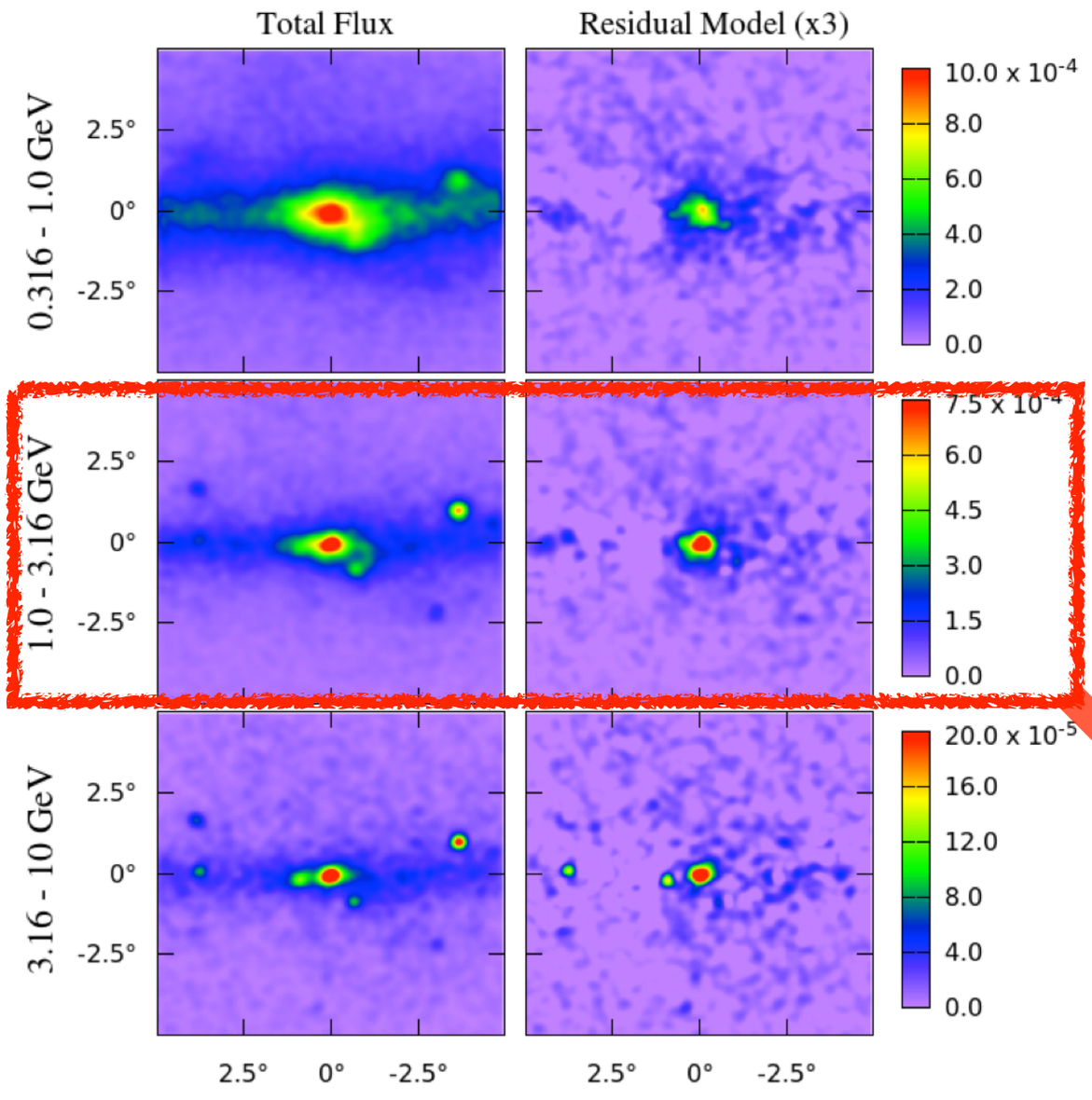

[1402.6703, T. Daylan et.al.]

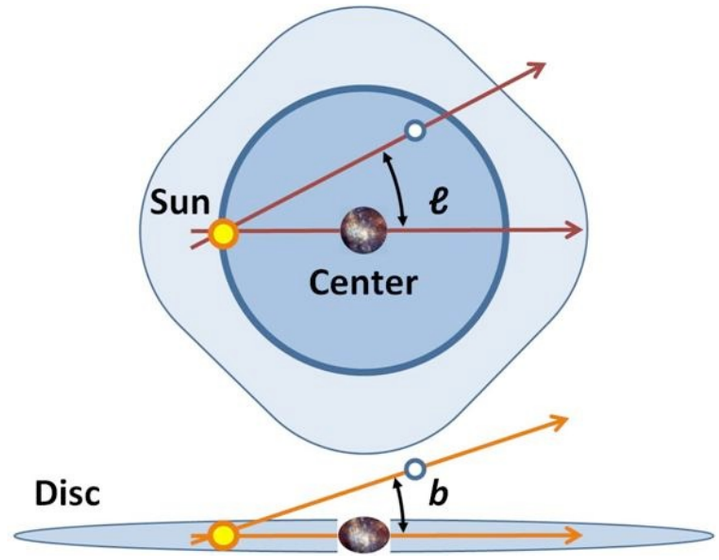

$$\mathrm{GC}: b \sim l \lesssim 0.1^\circ$$

extended
GeV scale excess!

- A DM interpretation

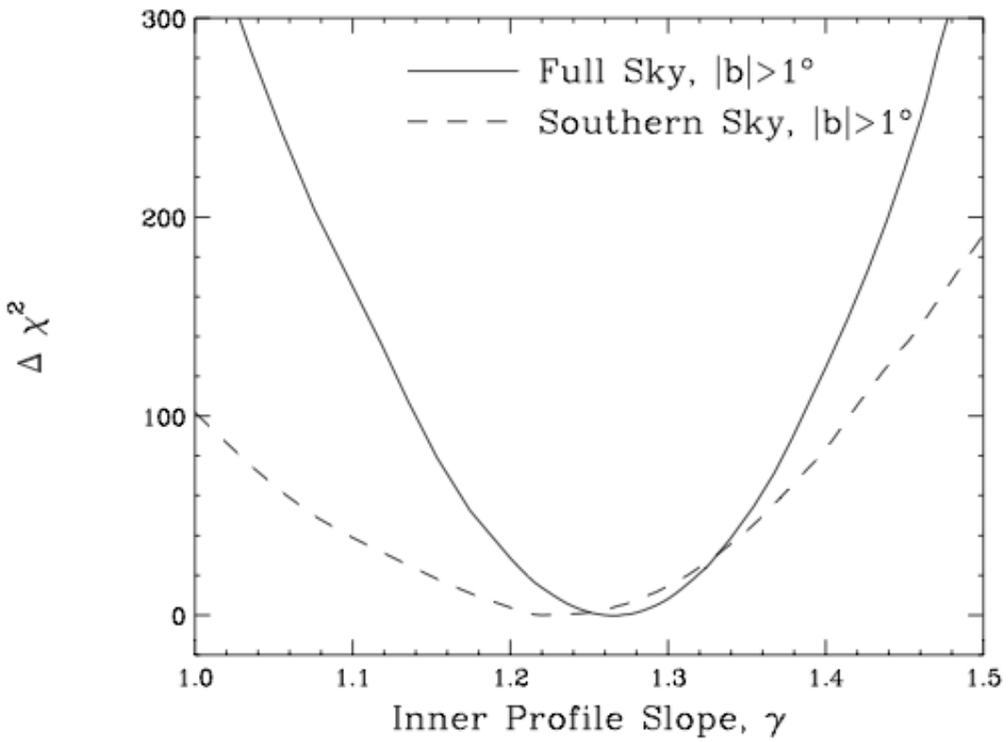

$\mathrm{DM} + \mathrm{DM} \to b\bar{b}$ with $\sigma v = 1.7 \times 10^{-26} \mathrm{cm}^3/\mathrm{s}$

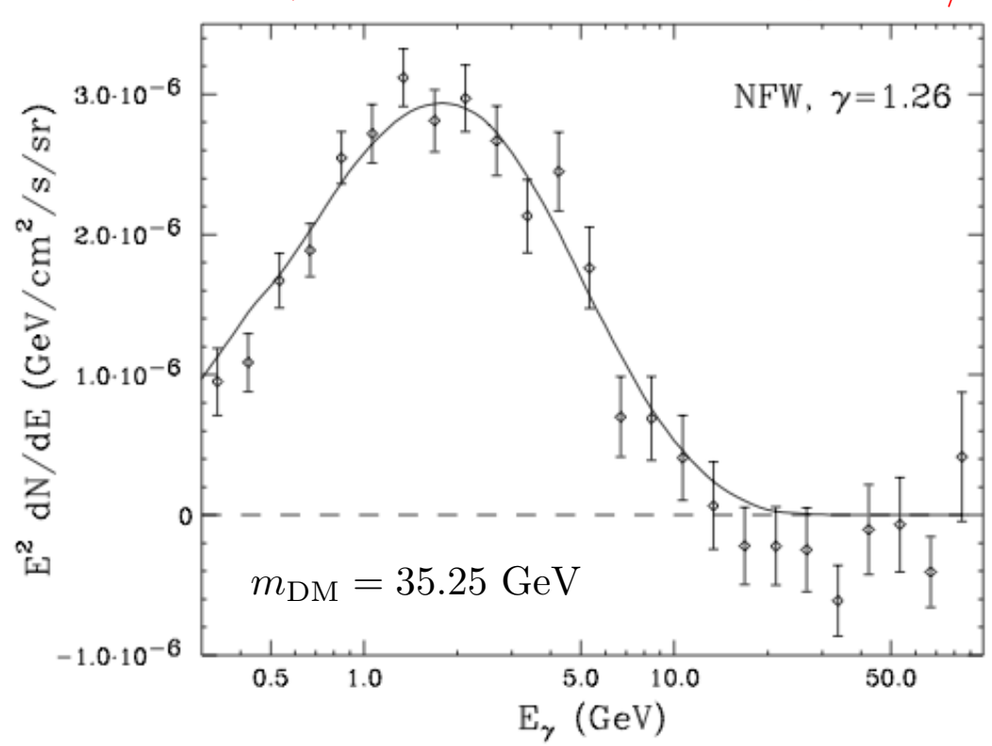

* See "1402.6703, T. Daylan et.al." for other possible channels

- Millisecond Pulars (astrophysical alternative)

It may or may not be the main source, depending on

- luminosity func.
- bulge population
- distribution of bulge population

* See "1404.2318, Q. Yuan & B. Zhang" and "1407.5625, I. Cholis, D. Hooper & T. Linden"

GC gamma ray in HP VDM

P. Ko, WI Park, Y. Tang. arXiv:1404.5257, JCAP

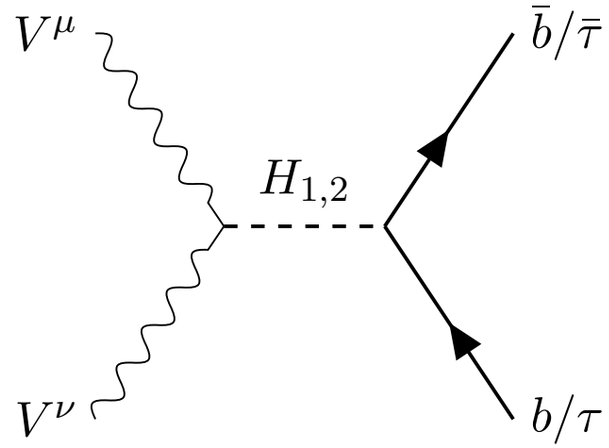

H2 : 125 GeV Higgs
H1 : absent in EFT

Figure 2. Dominant s channel $b + \bar{b}$ (and $\tau + \bar{\tau}$) production

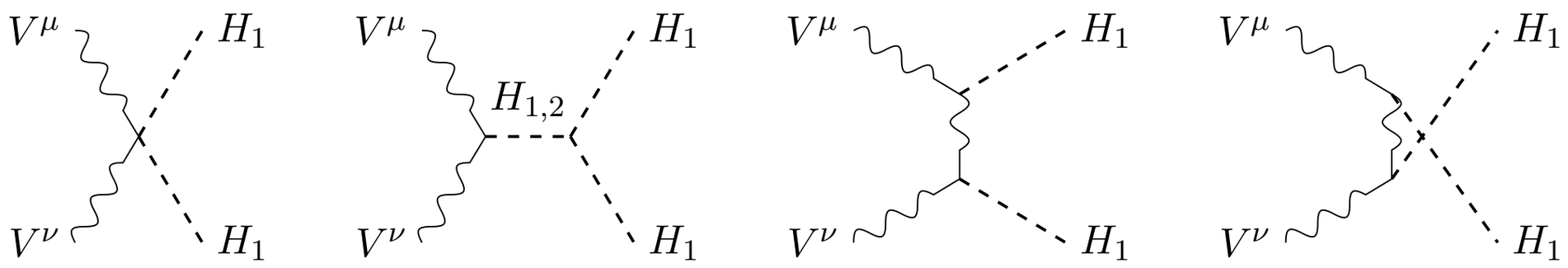

Figure 3. Dominant s/t-channel production of H_1s that decay dominantly to $b + \bar{b}$

Importance of HP VDM with Dark Higgs Boson

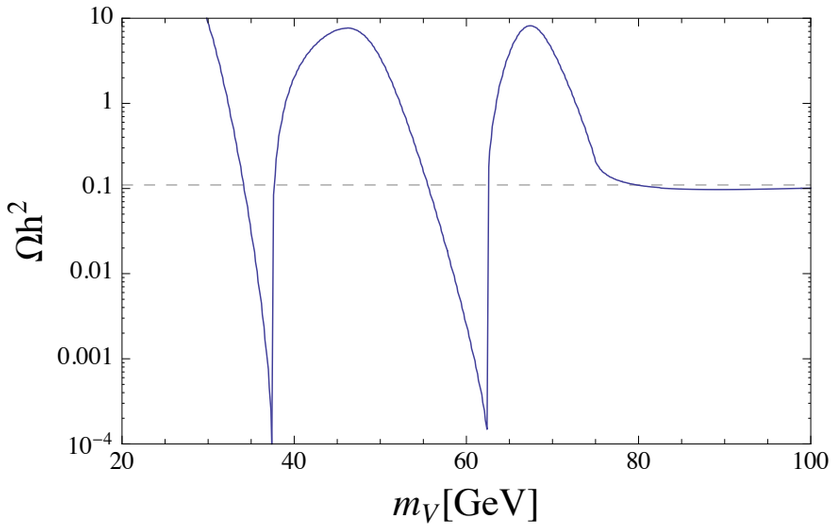

Figure 4. Relic density of dark matter as function of m_ψ for $m_h = 125$, $m_\phi = 75\,\mathrm{GeV}$, $g_X = 0.2$, and $\alpha = 0.1$.

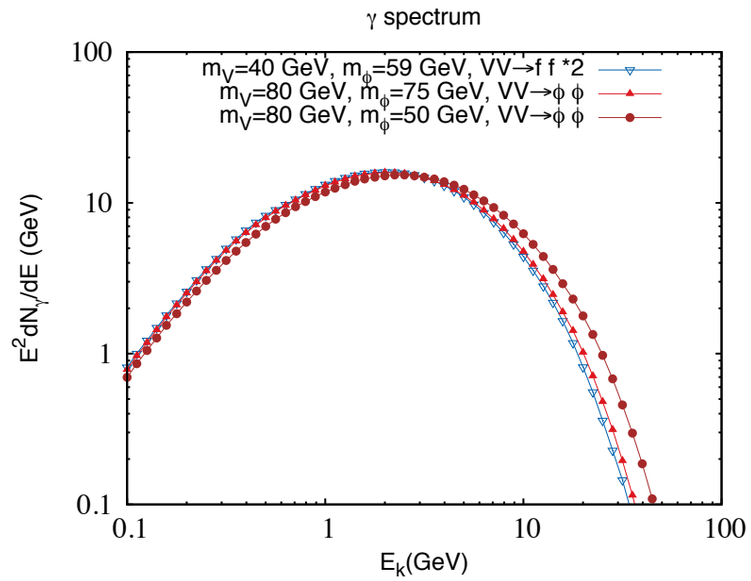

Figure 5. Illustration of γ spectra from different channels. The first two cases give almost the same spectra while in the third case γ is boosted so the spectrum is shifted to higher energy.

This mass range of VDM would have been impossible in the VDM model (EFT)

And No 2nd neutral scalar (Dark Higgs) in EFT

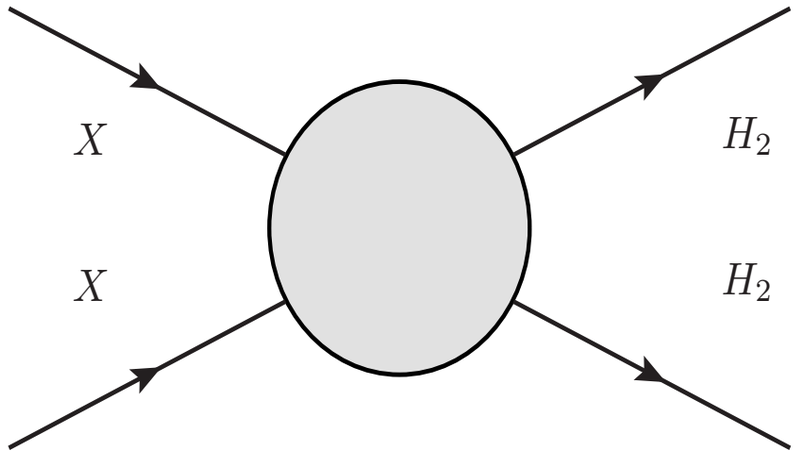

P.Ko, Yong Tang.
arXiv:1504.03908

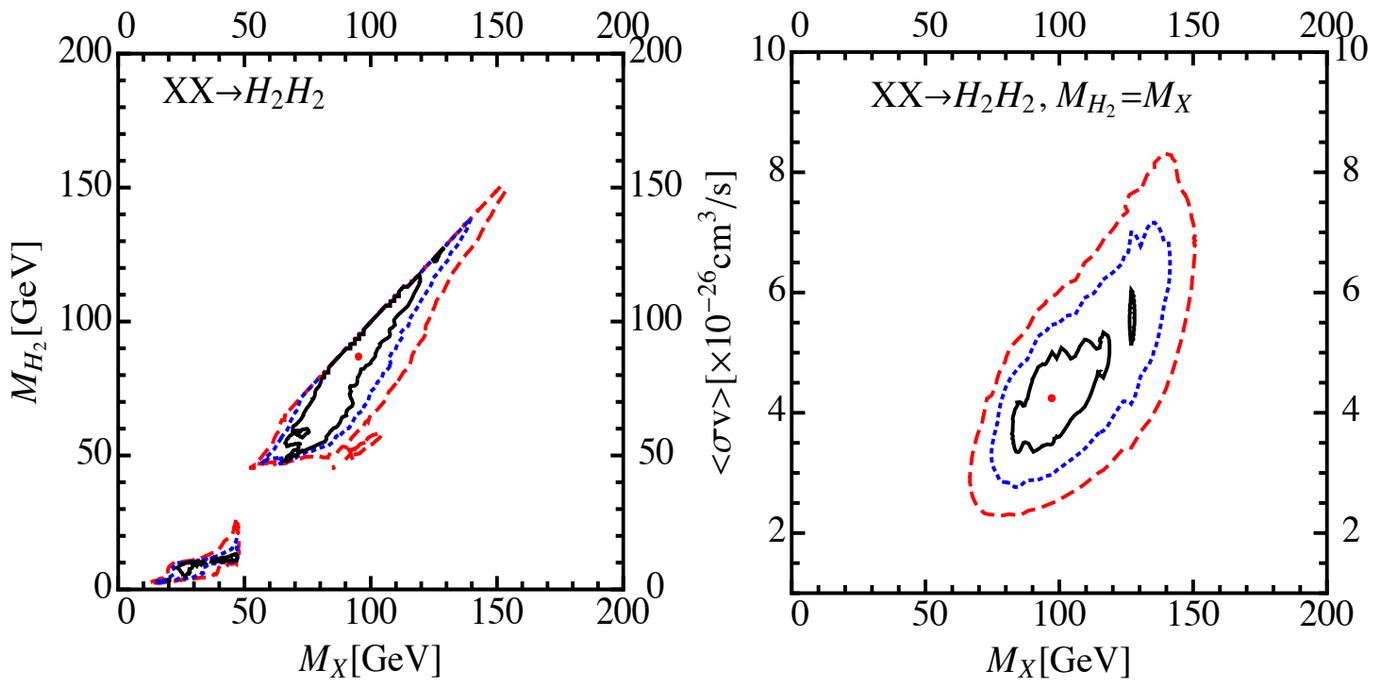

FIG. 3: The regions inside solid(black), dashed(blue) and long-dashed(red) contours correspond to 1σ, 2σ and 3σ, respectively. The red dots inside 1σ contours are the best-fit points. In the left panel, we vary freely M_X, M_{H_2} and $\langle\sigma v\rangle$. While in the right panel, we fix the mass of H_2, $M_{H_2} \simeq M_X$.

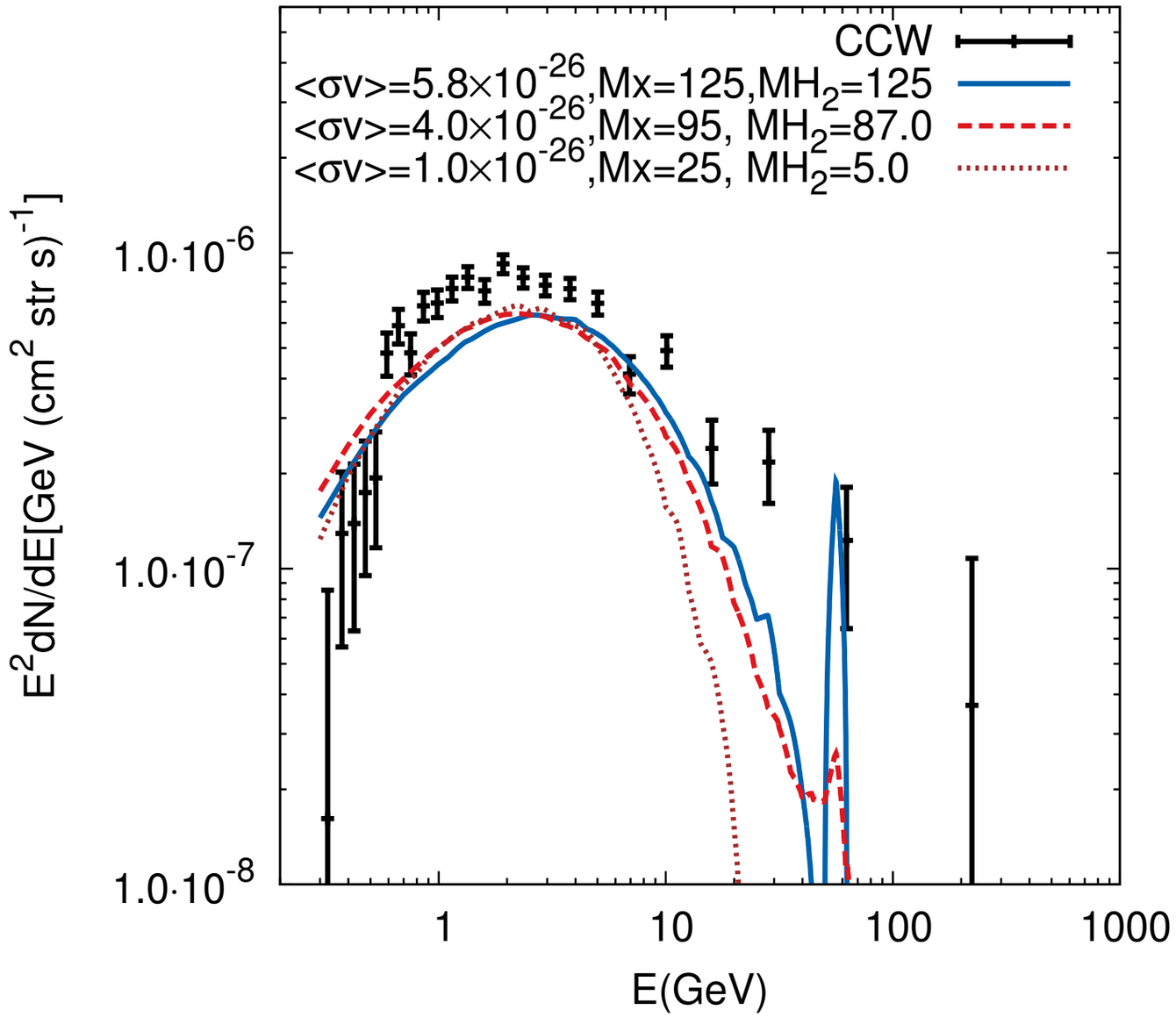

FIG. 2: Three illustrative cases for gamma-ray spectra in contrast with CCW data points [11]. All masses are in GeV unit and σv with cm^3/s. Line shape around $E \simeq M_{H_2}/2$ is due to decay modes, $H_2 \to \gamma\gamma, Z\gamma$.

This would have never been possible within the DM EFT

P.Ko, Yong Tang.
arXiv:1504.03908

Channels	Best-fit parameters	$\chi^2_{\rm min}$/d.o.f.	p-value
$XX \to H_2H_2$ (with $M_{H_2} \neq M_X$)	$M_X \simeq 95.0\text{GeV}, M_{H_2} \simeq 86.7\text{GeV}$ $\langle\sigma v\rangle \simeq 4.0 \times 10^{-26}\text{cm}^3/\text{s}$	22.0/21	0.40
$XX \to H_2H_2$ (with $M_{H_2} = M_X$)	$M_X \simeq 97.1\text{GeV}$ $\langle\sigma v\rangle \simeq 4.2 \times 10^{-26}\text{cm}^3/\text{s}$	22.5/22	0.43
$XX \to H_1H_1$ (with $M_{H_1} = 125\text{GeV}$)	$M_X \simeq 125\text{GeV}$ $\langle\sigma v\rangle \simeq 5.5 \times 10^{-26}\text{cm}^3/\text{s}$	24.8/22	0.30
$XX \to b\bar{b}$	$M_X \simeq 49.4\text{GeV}$ $\langle\sigma v\rangle \simeq 1.75 \times 10^{-26}\text{cm}^3/\text{s}$	24.4/22	0.34

TABLE I: Summary table for the best fits with three different assumptions.

DM Production @ ILC

P Ko, H Yokoya, arXiv:1603.08802, JHEP

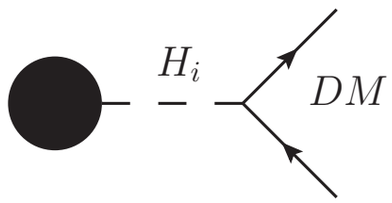

,

$$t \equiv m_{DD}^2$$

We consider $e^+e^- \to Z* \to ZH_{i=1,2}$ followed by $H_i \to \bar{\chi}\chi$

$$\frac{d\sigma_{\rm SDM}}{dt} \propto \sigma^{h*}_{\rm SDM} \times |\frac{1}{t-m_h^2+im_h\Gamma_h}|^2,$$

$$\frac{d\sigma_{\rm FDM}}{dt} \propto \sigma^{h*}_{\rm FDM} \times |\frac{1}{t-m_{H_1}^2+im_{H_1}\Gamma_{H_1}} - \frac{1}{t-m_{H_2}^2+im_{H_2}\Gamma_{H_2}}|^2 \cdot \left(2t-8m_\chi^2\right),$$

$$\frac{d\sigma_{\rm VDM}}{dt} \propto \sigma^{h*}_{\rm VDM} \times |\frac{1}{t-m_{H_1}^2+im_{H_1}\Gamma_{H_1}} - \frac{1}{t-m_{H_2}^2+im_{H_2}\Gamma_{H_2}}|^2 \cdot \left(2+\frac{(t-2m_D^2)^2}{4m_V^4}\right).$$

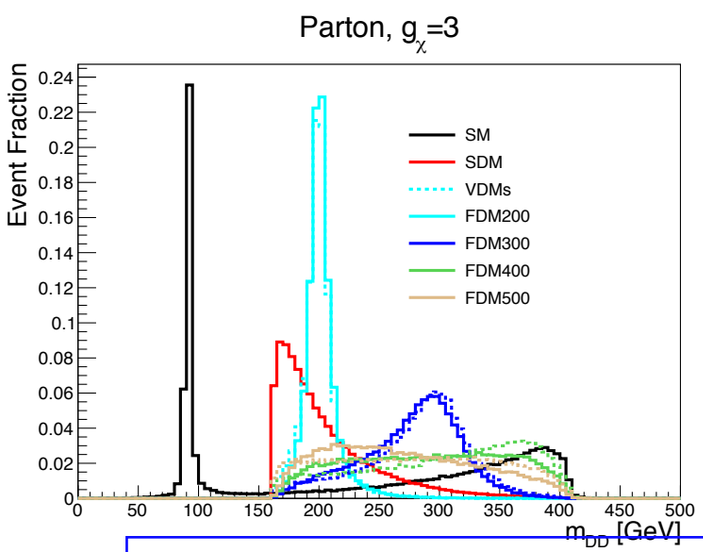

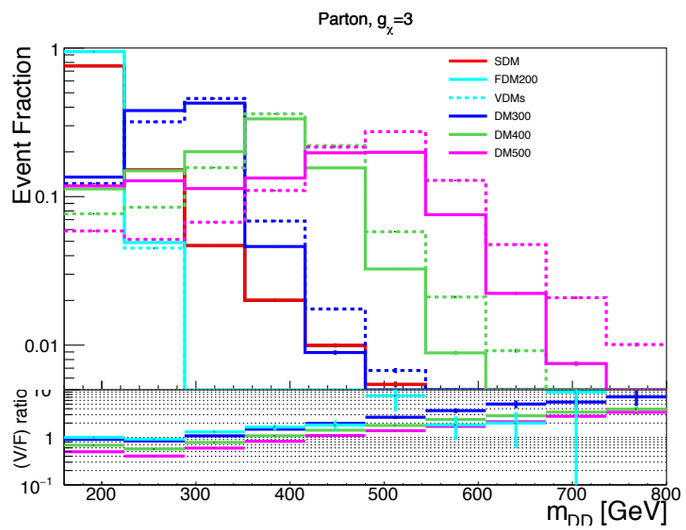

Fix DM mass = 80 GeV, sin(alpha) = 0.3, and vary H2 mass (200,300,400,500) GeV

Asymptotic behavior in the full theory ($t \equiv m^2_{\chi\chi}$)

$$\text{ScalarDM}: \quad G(t) \sim \frac{1}{(t-m_H^2)^2 + m_H^2\Gamma_H^2} \tag{5.7}$$

$$\text{SFDM}: \quad G(t) \sim \left|\frac{1}{t-m_1^2+im_1\Gamma_1} - \frac{1}{t-m_2^2+im_2\Gamma_2}\right|^2 \ (t-4m_\chi^2) \tag{5.8}$$

$$\to |\frac{1}{t^2}|^2 \times t \sim \frac{1}{t^3} \ (\text{as } t\to\infty) \tag{5.9}$$

$$\text{VDM}: \quad G(t) \sim \left|\frac{1}{t-m_1^2+im_1\Gamma_1} - \frac{1}{t-m_2^2+im_2\Gamma_2}\right|^2 \ \left[2+\frac{(t-2m_V^2)^2}{4m_V^4}\right] \tag{5.10}$$

$$\to |\frac{1}{t^2}|^2 \times t^2 \sim \frac{1}{t^2} \ (\text{as } t\to\infty) \tag{5.11}$$

Asymptotic behavior w/o the 2nd Higgs (EFT)

$$\text{SFDM}: \quad G(t) \sim \frac{1}{(t-m_H^2)^2 + m_H^2\Gamma_H^2} \ (t-4m_\chi^2)$$

$$\to \frac{1}{t} \ (\text{as } t\to\infty)$$

$$\text{VDM}: \quad G(t) \sim \frac{1}{(t-m_H^2)^2 + m_H^2\Gamma_H^2} \ \left[2+\frac{(t-2m_V^2)^2}{4m_V^4}\right]$$

$$\to \text{constant} \ (\text{as } t\to\infty)$$

Unitarity is violated in EFT!

Summary

- Phenomenology of HP VDM and Singlet FDM presented within EFT vs. UV completed models

- EFT approach has a number of drawbacks : non-renormalizable, unitarity violation at high energy colliders, and it applies only if $m_{DM}, m_{\rm SM} \ll m_\phi$ [We don't know mass scales of dark particles]

- In particular, one has $\Gamma_{\rm EFT}(H_{125} \to VV) \to \infty$, as $m_V \to 0$, whereas it is finite in UV completed models [Importance of gauge invariance, unitarity and renormalizability]

- The dark Higgs ϕ can play crucial roles in interpreting the DM signatures at colliders, explaining the GC γ-ray excess ($VV \to \phi\phi$), improving vacuum stability up to Planck scale, modifying the Higgs inflation [ϕ should be actively searched for !]

XENON1T Excess

(Scalar XDM, Fermion XDM)

XENON1T Excess

- Excess between 1-7 keV
  - Expectated : 232 ± 15 , Observed : 285
  - Deviation ~ 3.5 σ
- Tritium contamination
  - Long half lifetime (12.3 years)
  - Abundant in atmosphere and cosmogenically produced in Xenon
- Solar axion
  - Produced in the Sun
  - Favored over bkgd @ 3.5 σ
- Neutrino magnetic dipole moment
  - Favored @ 3.2 σ

Electron recoil

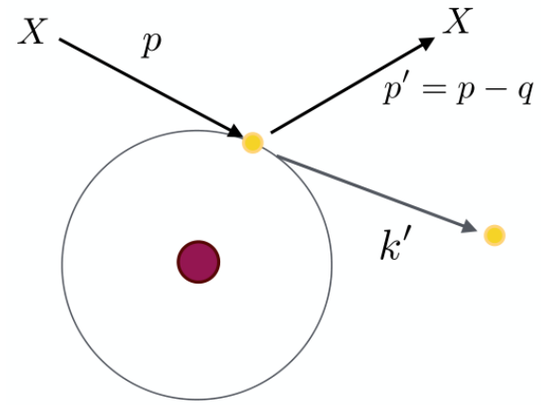

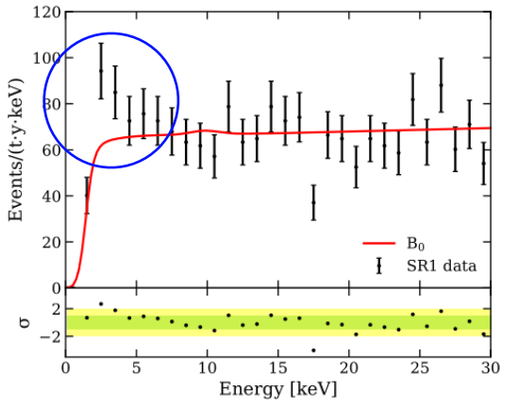

DD/CMB Constraints

- To evade stringent bounds from direct detection expt's : sub GeV DM

- CMB bound excludes thermal DM freeze-out determined by S-wave annihilation : DM annihiliation should be mainly in P-wave $\langle \sigma v \rangle \sim \cancel{a} + bv^2$

Planck 2018
R.K.Leane 35 al, PRD2018

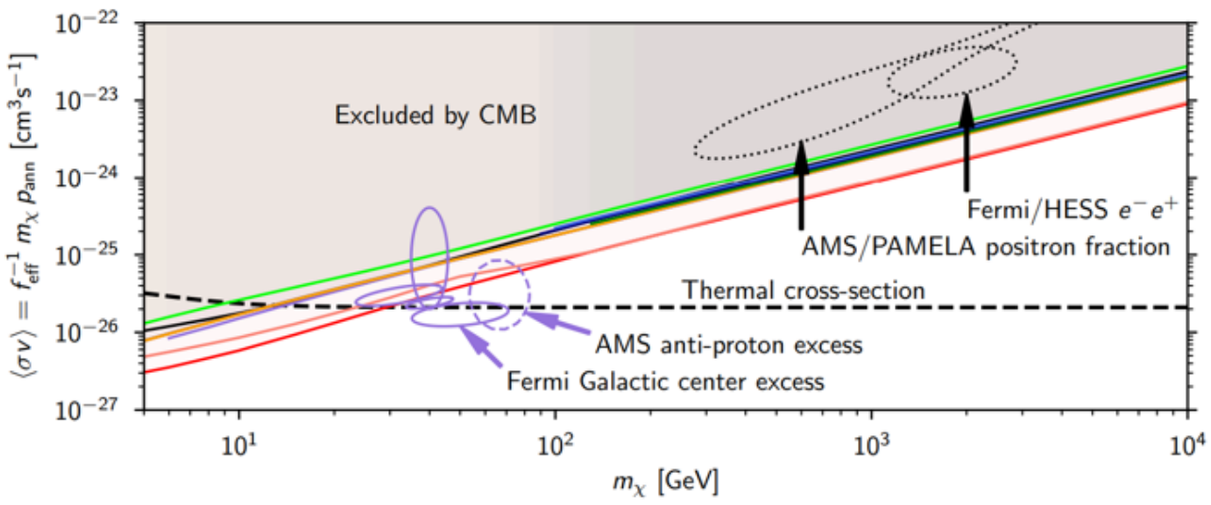

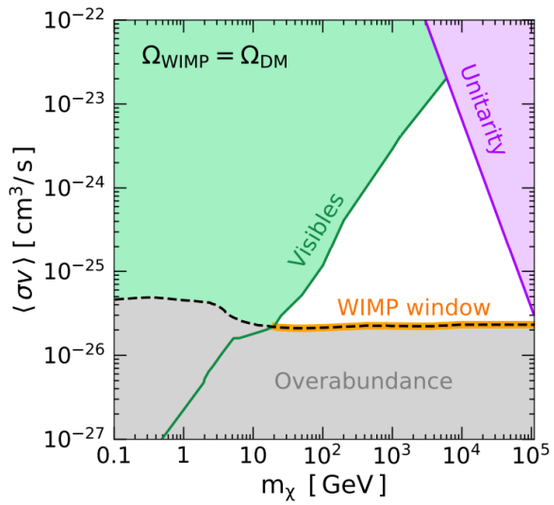

Exothermic DM

- Inelastic exothermic scattering of XDM
- $XDM + e_{\text{atomic}} \rightarrow DM + e_{\text{free}}$ by dark photon exchange + kinetic mixing
- Excess is determined by $E_R \sim \delta = m_{XDM} - m_{DM}$
- Most works are based on effective/toy models where δ is put in by hand, or ignored dark Higgs
- dim-2 op for scalar DM and dim-3 op for fermion DM : soft and explicit breaking of local gauge symmetry), and include massive dark photon as well $\rightarrow$ theoretically inconsistent !

Z_2 DM models with dark Higgs

- We solve this inconsistency and unitarity issue with Krauss-Wilczek mechanism

- By introducing a dark Higgs, we have many advantages:

  - Dark photon gets massive

  - Mass gap δ is generated by dark Higgs mechanism

  - We can have DM pair annihilation in P-wave involving dark Higgs in the final states, unlike in other works

Usual Approaches

For example, Harigaya, Nagai, Suzuki, arXiv:2006.11938

$$V(\phi) = m^2|\phi|^2 + \Delta^2\left(\phi^2 + \phi^{*2}\right), \qquad (1)$$

This term is problematic

$$\mathcal{L} = g_D A'^{\mu}\left(\chi_1 \partial_\mu \chi_2 - \chi_2 \partial_\mu \chi_1\right) + \epsilon e A'_\mu J^\mu_{\rm EM},$$

Similarly for the fermion DM case

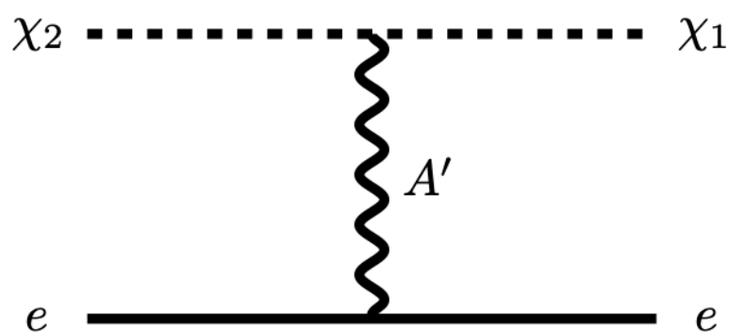

FIG. 1. Inelastic scattering of the heavier DM particle χ_2 off the electron e into the lighter particle χ_1, mediated by the dark photon A'.

- The model is not mathematically consistent, since there is no conserved current a dark photon can couple to in the massless limit
- The second term with Δ^2 breaks $U(1)_X$ explicitly, although softly

Relic Density from

$$XX^{\dagger} \to Z^{'\,*} \to f\bar{f}$$

(P-wave annihilation)

For example, Harigaya, Nagai, Suzuki, arXiv:2006.11938

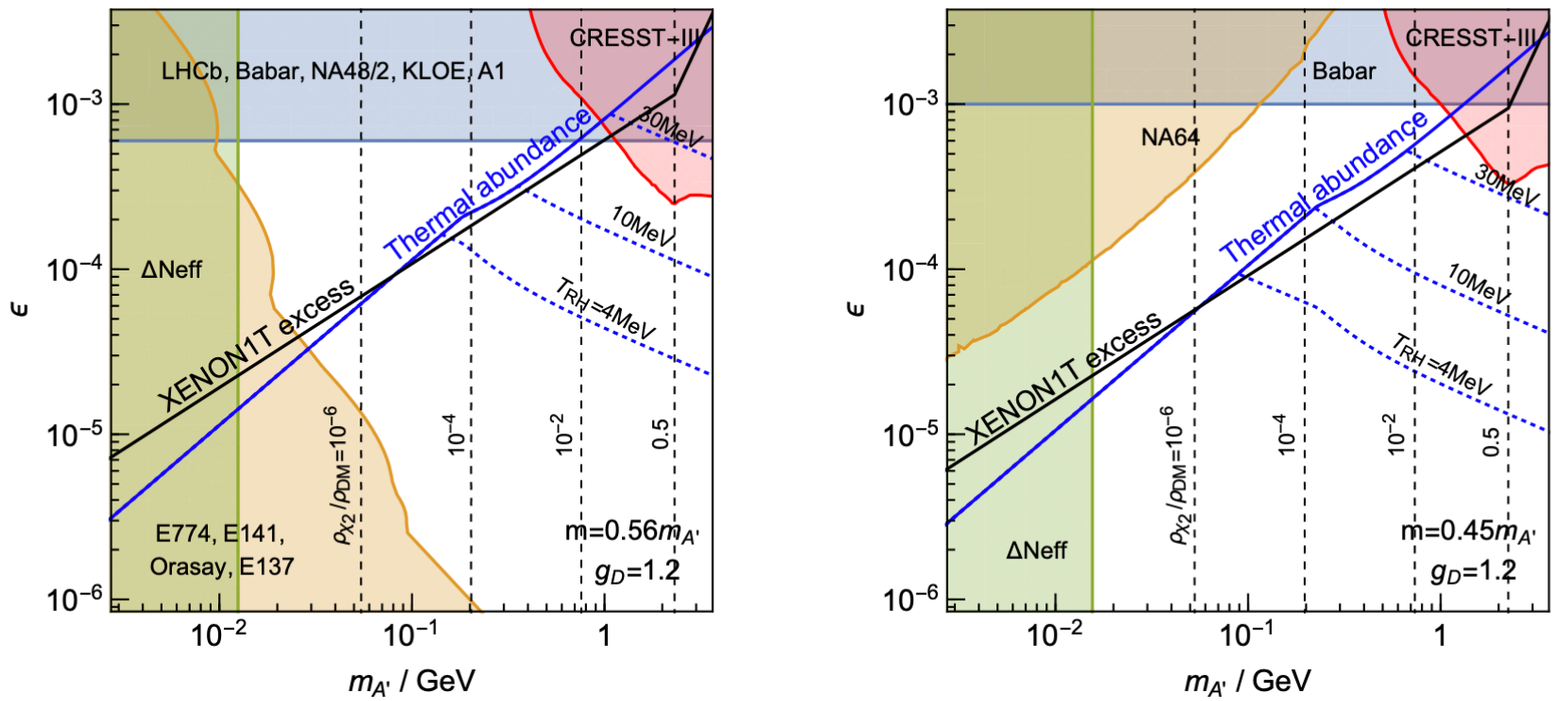

FIG. 4. The required value of ϵ to explain the observed excess of events at XENON1T in terms of the dark photon mass $m_{A'}$ (black solid lines). The left and right panels correspond to the cases of $m > m_{A'}/2$ and $m < m_{A'}/2$ respectively. We assume $g_D = 1.2$ in both cases. The blue lines denote the required value of ϵ to obtain the observed DM abundance by the thermal freeze-out process, discussed in Sec. IV. The solid lines correspond to the case without any entropy production. The dashed lines assume freeze-out during a matter dominated era and the subsequent reheating at $T_{\rm RH}$, which suppresses the DM abundance by a factor of $(T_{\rm RH}/T_{\rm FO})^3$. The black dashed lines denote the mass density of χ_2 normalized by the total DM density. The shaded regions show the constraints from dark radiation and various searches for the dark photon A' which are discussed in Sec. V.

Scalar XDM (X_R & X_I)

Field	ϕ	X	χ
U(1) charge	2	1	1

$$\mathcal{L} = \mathcal{L}_{\rm SM} - \frac{1}{4}\hat{X}_{\mu\nu}\hat{X}^{\mu\nu} - \frac{1}{2}\sin\epsilon\hat{X}_{\mu\nu}\hat{B}^{\mu\nu} + D^\mu\phi^\dagger D_\mu\phi + D^\mu X^\dagger D_\mu X - m_X^2 X^\dagger X + m_\phi^2\phi^\dagger\phi$$
$$-\lambda_\phi\left(\phi^\dagger\phi\right)^2 - \lambda_X\left(X^\dagger X\right)^2 - \lambda_{\phi X}X^\dagger X\phi^\dagger\phi - \lambda_{\phi H}\phi^\dagger\phi H^\dagger H - \lambda_{HX}X^\dagger X H^\dagger H$$
$$-\mu\left(X^2\phi^\dagger + H.c.\right), \qquad (1)$$

$$X = \frac{1}{\sqrt{2}}(X_R + iX_I),$$

$$H = \begin{pmatrix} 0 \\ \frac{1}{\sqrt{2}}(v_H + h_H) \end{pmatrix}, \quad \phi = \frac{1}{\sqrt{2}}(v_\phi + h_\phi),$$

$$\mathcal{L} \supset \epsilon g_X s_W Z^\mu(X_R\partial_\mu X_I - X_I\partial_\mu X_R) - \frac{g_Z}{2}Z_\mu\overline{\nu}_L\gamma^\mu\nu_L,$$

$$\mathcal{L} \supset g_X Z'^\mu(X_R\partial_\mu X_I - X_I\partial_\mu X_R) - \epsilon\, e c_W Z'_\mu\overline{e}\gamma^\mu e,$$

$U(1) \to Z_2$ by $v_\phi \neq 0 : X \to -X$

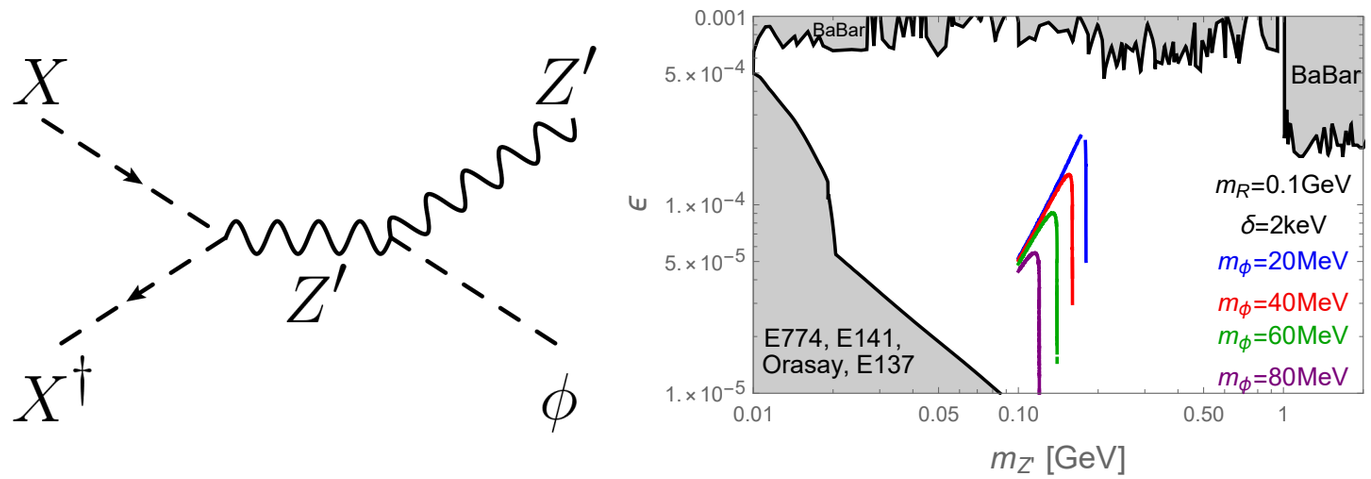

FIG. 1: (*left*) Feynman diagrams relevant for thermal relic density of DM: $XX^\dagger \to Z'\phi$ and (*right*) the region in the $(m_{Z'}, \epsilon)$ plane that is allowed for the XENON1T electron recoil excess and the correct thermal relic density for scalar DM case for $\delta = 2$ keV : (a) $m_{\rm DM} = 0.1$ GeV. Different colors represents $m_\phi = 20, 40, 60, 80$ MeV. The gray areas are excluded by various experiments, from BaBar [61], E774 [62], E141 [63], Orasay [64], and E137 [65], assuming $Z' \to X_R X_I$ is kinematically forbidden.

P-wave annihilation x-sections

Scalar DM : $XX^{\dagger} \rightarrow Z^{'*} \rightarrow Z^{'}\phi$

$$\sigma v \simeq \frac{g_X^4 v^2}{384\pi\, m_X^4 (4m_X^2 - m_{Z'}^2)^2} \left(16m_X^4 + m_{Z'}^4 + m_\phi^4 + 40m_X^2 m_{Z'}^2 - 8m_X^2 m_\phi^2 - 2m_{Z'}^2 m_\phi^2\right)$$
$$\times \left[\left\{4m_X^2 - (m_{Z'} + m_\phi)^2\right\}\left\{4m_X^2 - (m_{Z'} - m_\phi)^2\right\}\right]^{1/2} + \mathcal{O}(v^4), \qquad (10)$$

Fermion XDM (χ_R & χ_I)

$$\begin{aligned}\mathcal{L} &= -\frac{1}{4}\hat{X}^{\mu\nu}\hat{X}_{\mu\nu} - \frac{1}{2}\sin\epsilon\hat{X}_{\mu\nu}B^{\mu\nu} + \overline{\chi}\left(i\not{D} - m_\chi\right)\chi + D_\mu\phi^\dagger D^\mu\phi \\ &- \mu^2\phi^\dagger\phi - \lambda_\phi|\phi|^4 - \frac{1}{\sqrt{2}}\left(y\phi^\dagger\overline{\chi^C}\chi + \text{h.c.}\right) - \lambda_{\phi H}\phi^\dagger\phi H^\dagger H\end{aligned}$$

$$\begin{aligned}\chi &= \frac{1}{\sqrt{2}}(\chi_R + i\chi_I), \\ \chi^c &= \frac{1}{\sqrt{2}}(\chi_R - i\chi_I), \\ \chi_R^c &= \chi_R, \quad \chi_I^c = \chi_I,\end{aligned}$$

$$\begin{aligned}\mathcal{L} &= \frac{1}{2}\sum_{i=R,I}\overline{\chi_i}\left(i\not{\partial} - m_i\right)\chi_i - i\frac{g_X}{2}(Z'_\mu + \epsilon s_W Z_\mu)\left(\overline{\chi_R}\gamma^\mu\chi_I - \overline{\chi_I}\gamma^\mu\chi_R\right) \\ &- \frac{1}{2}yh_\phi\left(\overline{\chi_R}\chi_R - \overline{\chi_I}\chi_I\right),\end{aligned}$$

$U(1) \to Z_2$ by $v_\phi \neq 0 : \chi \to -\chi$

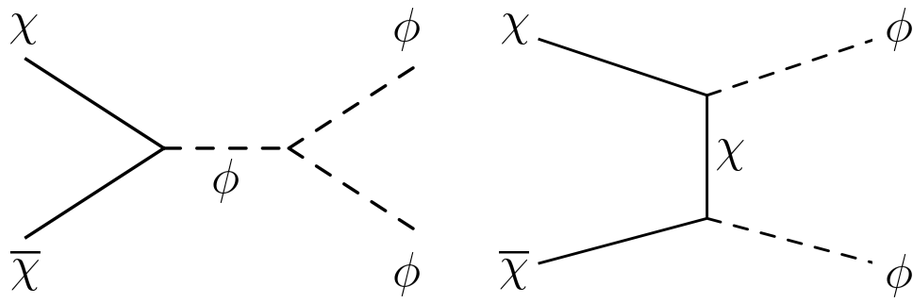

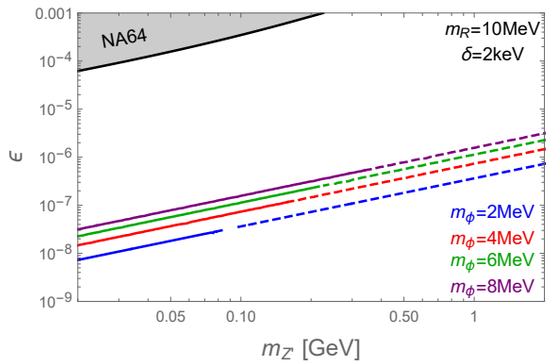

FIG. 2: (*top*) Feyman diagrams for $\chi\bar{\chi} \to \phi\phi$. (*bottom*) the region in the $(m_{Z'}, \epsilon)$ plane that is allowed for the XENON1T electron recoil excess and the correct thermal relic density for fermion DM case for $\delta = 2$ keV and the fermion DM mass to be $m_R = 10$ MeV. Different colors represents $m_\phi = 2, 4, 6, 8$ MeV. The gray areas are excluded by various experiments, assuming $Z' \to \chi_R \chi_I$ is kinematically allowed, and the experimental constraint is weaker in the ϵ we are interested in, compared with the scalar DM case in Fig. 1 (right). We also show the current experimental bounds by NA64 [66].

P-wave annihilation x-sections

Scalar DM : $XX^\dagger \to Z'^* \to Z'\phi$

$$\sigma v \simeq \frac{g_X^4 v^2}{384\pi\, m_X^4 (4m_X^2 - m_{Z'}^2)^2} \left(16m_X^4 + m_{Z'}^4 + m_\phi^4 + 40m_X^2 m_{Z'}^2 - 8m_X^2 m_\phi^2 - 2m_{Z'}^2 m_\phi^2\right)$$
$$\times \left[\left\{4m_X^2 - (m_{Z'} + m_\phi)^2\right\}\left\{4m_X^2 - (m_{Z'} - m_\phi)^2\right\}\right]^{1/2} + \mathcal{O}(v^4), \qquad (10)$$

Fermion DM : $\chi\bar{\chi} \to \phi\phi$

$$\sigma v = \frac{y^2 v^2 \sqrt{m_\chi^2 - m_\phi^2}}{96\pi m_\chi}\left[\frac{27\lambda_\phi^2 v_\phi^2}{(4m_\chi^2 - m_\phi^2)^2} + \frac{4y^2 m_\chi^2 (9m_\chi^4 - 8m_\chi^2 m_\phi^2 + 2m_\phi^4)}{(2m_\chi^2 - m_\phi^2)^4}\right] + \mathcal{O}(v^4), \qquad (28)$$

Crucial to include “dark Higgs” to have DM pair annihilation in P-wave

$U(1)_{L_\mu - L_\tau}$ -charged DM

: Z' only vs. $Z' + \phi$

Work in preparation,
With Seungwon Baek, Jongkuk Kim

U M

PLOTS HERE

PRELIMINARY

Work in preparation,
With Seungwon Baek, Jongkuk Kim

Models with Φ

TABLE I: $U(1)$ charge assignments of newly introduced particles and SM particles. The other SM particles are singlet.

Field	Z'_μ	$X(\chi)$	Φ	$L_\mu = (\nu_{L\mu}, \mu_L), \mu_R$	$L_\tau = (\nu_{L\tau}, \tau_L), \tau_R$
spin	1	0 (1/2)	0	1/2	1/2
$U(1)$ charge	0	$Q_X(Q_\chi)$	Q_Φ	+1	-1

- Physics depends on Q_Φ , Q_X and Q_χ

- $Q_\Phi = 2Q_{X(\chi)}$ and $3Q_X$ need special cares, since there are extra gauge invariant op's that break $U(1) \to Z_2$, Z_3 after $U(1)$ is spontaneously broken by nonzero VEV of Φ

Complex Scalar DM (generic with $Q_\Phi \neq Q_X, etc$)

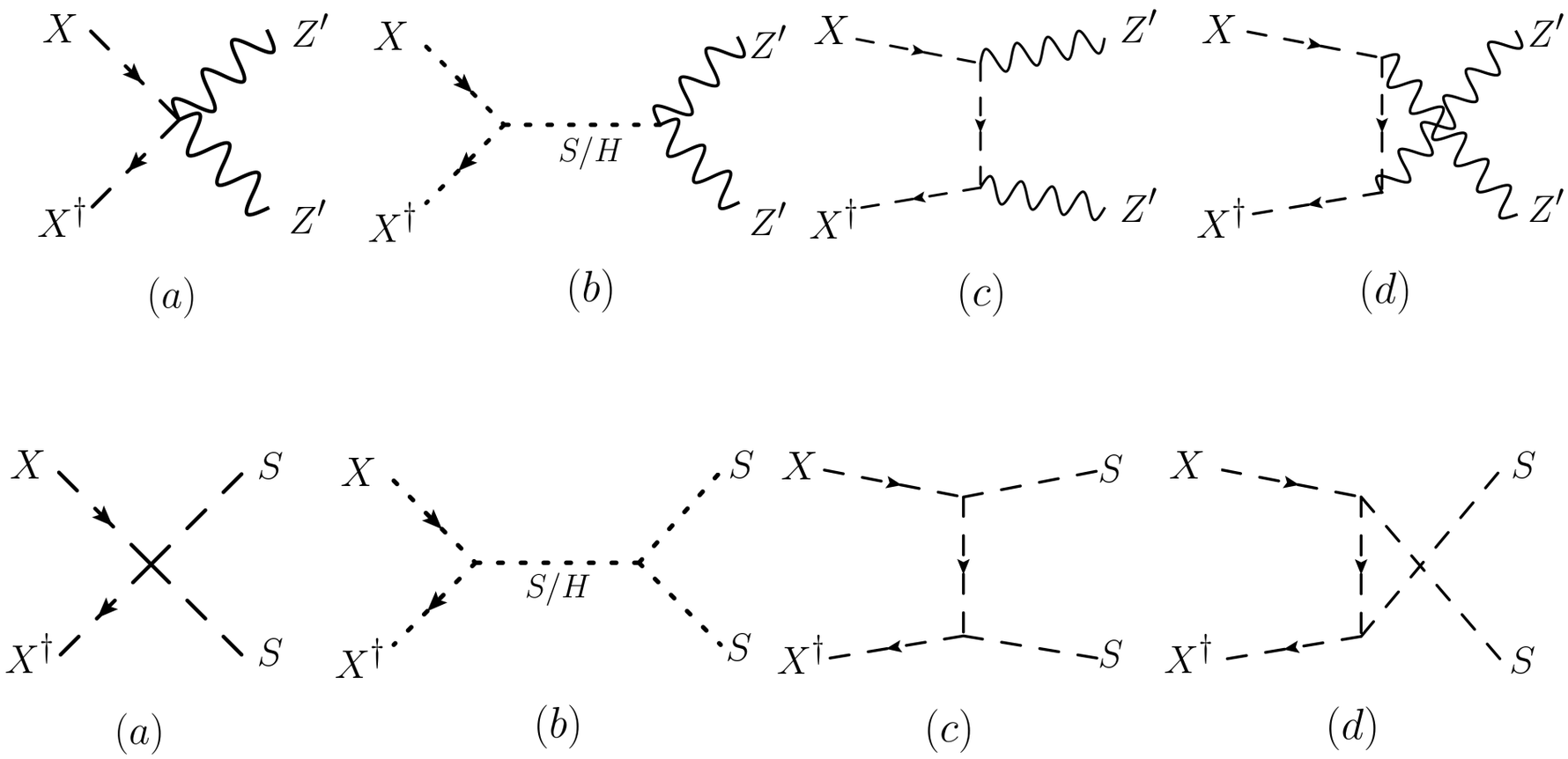

FIG. 2: (*Top*) Feynman diagrams for Complex scalar DM annihilatiing to a pair of Z' bosons. (*Bottom*) Feynman diagrams for Complex scalar DM annihilatiing to a pair of S bosons.

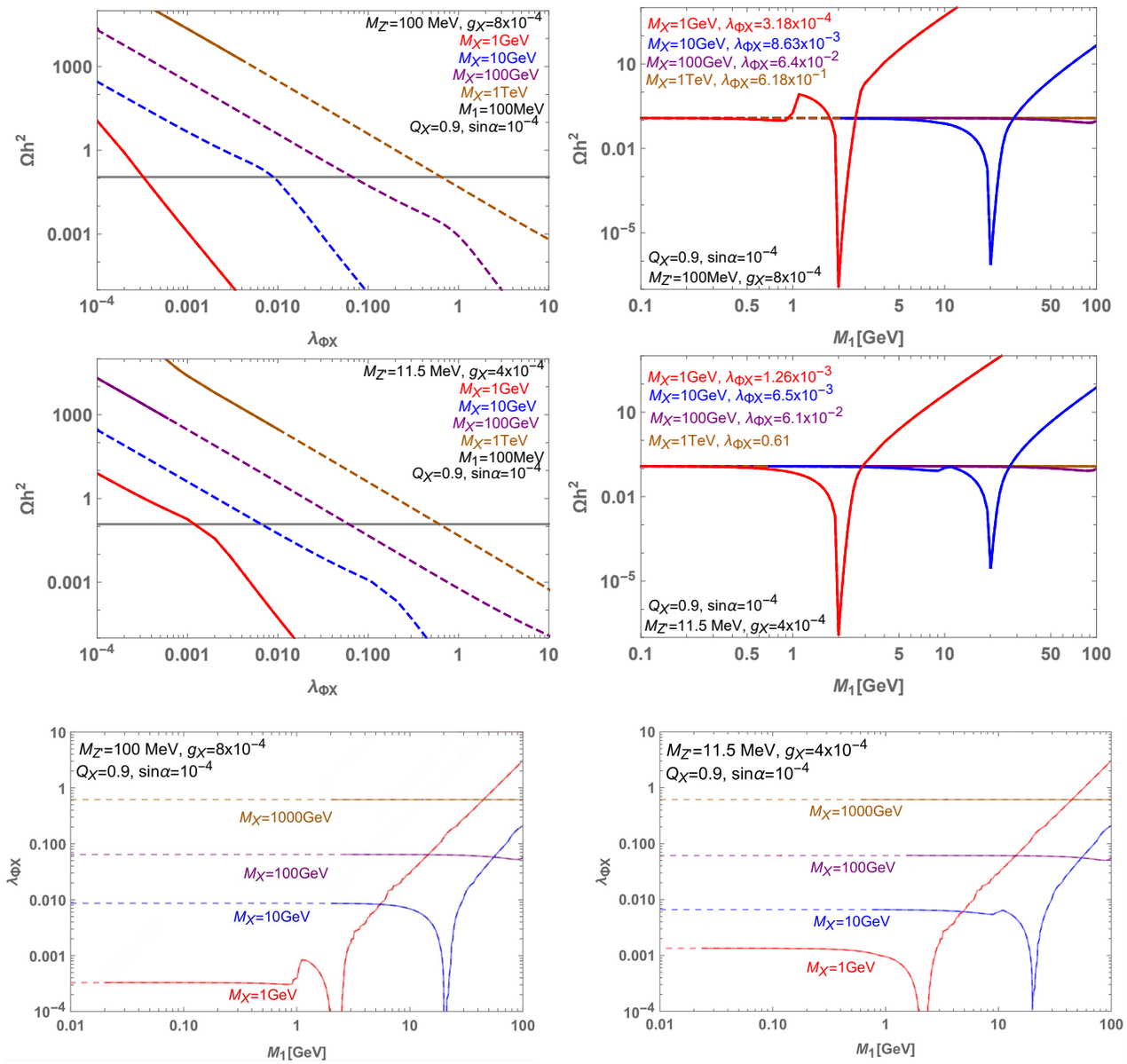

FIG. 3: Relic abundance of complex scalar DM. We take four different DM masses, 1, 10, 100, 1000GeV, respectively. (*Top*) We used $Q_\Phi = 1$, $Q_X = 0.9$, $M_{Z'} = 100$MeV and $g_X = 8 \times 10^{-4}$ as inputs. (*Middle*) We have set $Q_\Phi = 1$, $Q_X = 0.9$, $M_{Z'} = 11.5$MeV and $g_X = 4 \times 10^{-4}$ as inputs.(*Bottom*) Preferred paramater space in the $\lambda_{\Phi X} - M_1$ plane for $\lambda_{XH} = 0$. Solid (Dashed) lines represent the region where bounds on DM direct detection are satisfied (ruled out).

Complex Scalar DM:

$$U(1)_{L_\mu - L_\tau} \to Z_2 \; (Q_\Phi = 2Q_X)$$

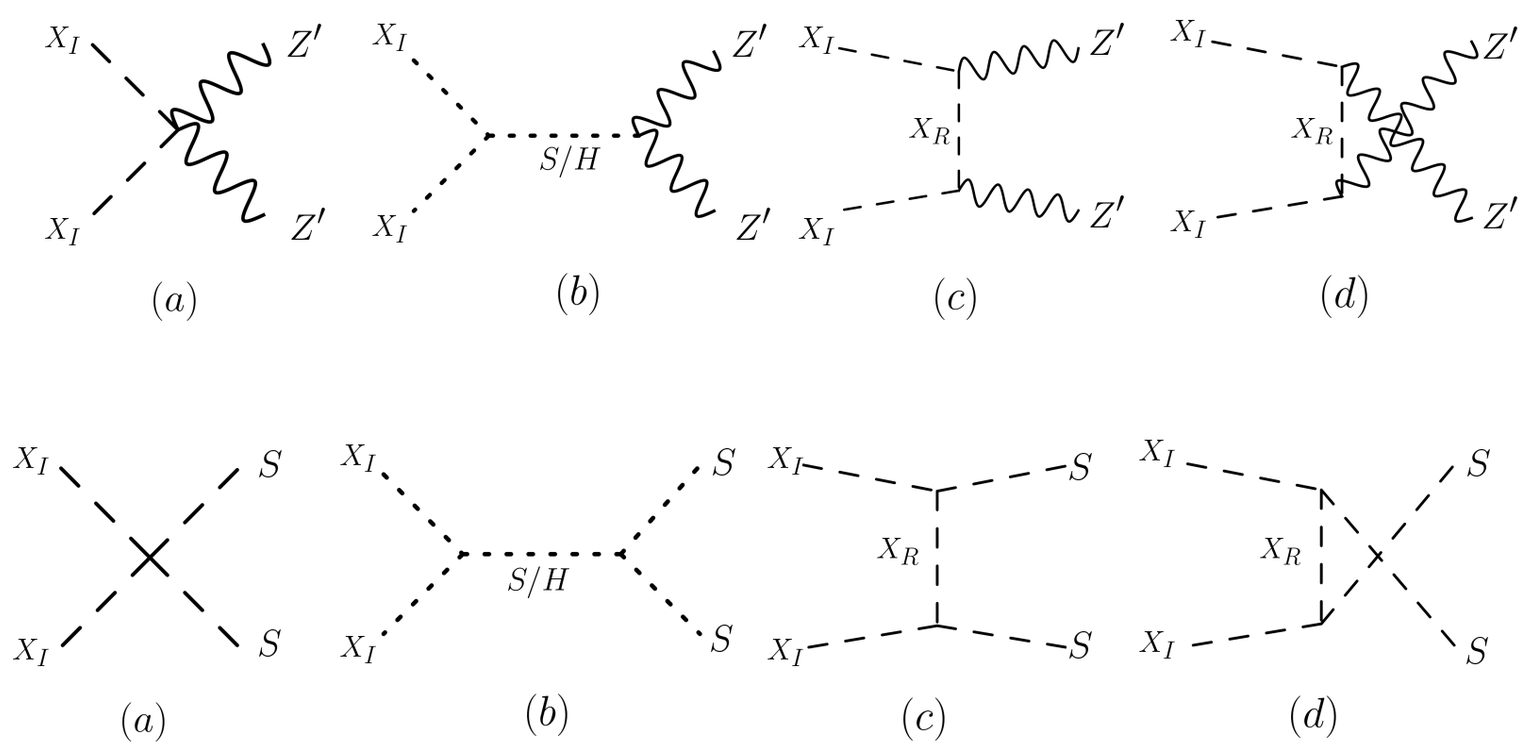

FIG. 5: (*Top*) Feynman diagrams for local Z_2 scalar DM annihilatiing to a pair of Z' bosons. (*Bottom*) Feynman diagrams for local Z_2 scalar DM annihilatiing to a pair of S bosons.

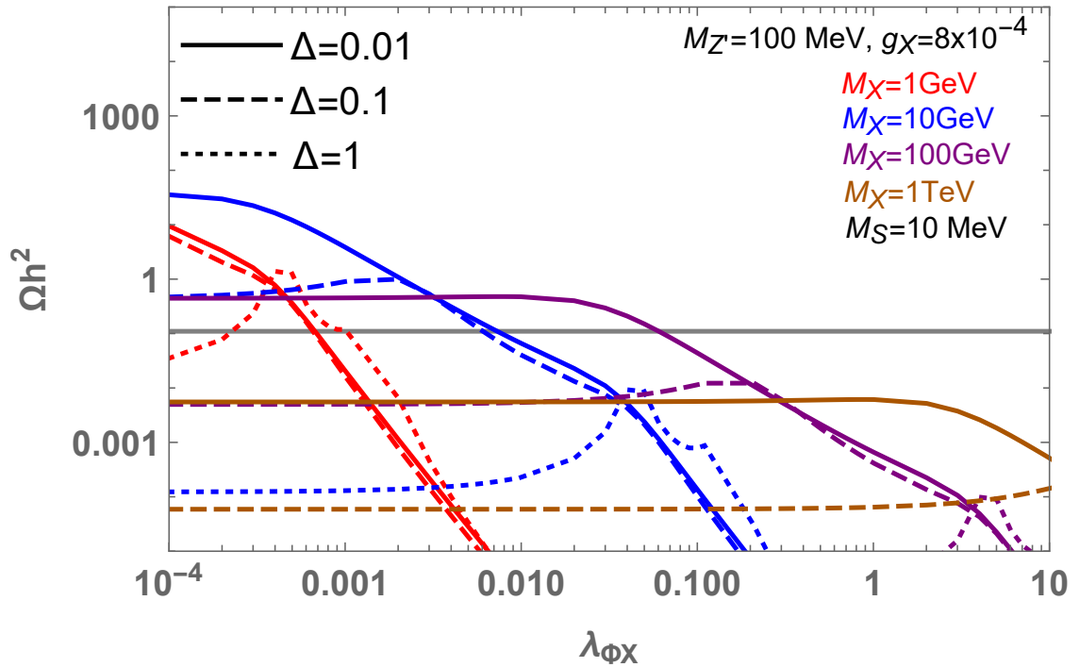

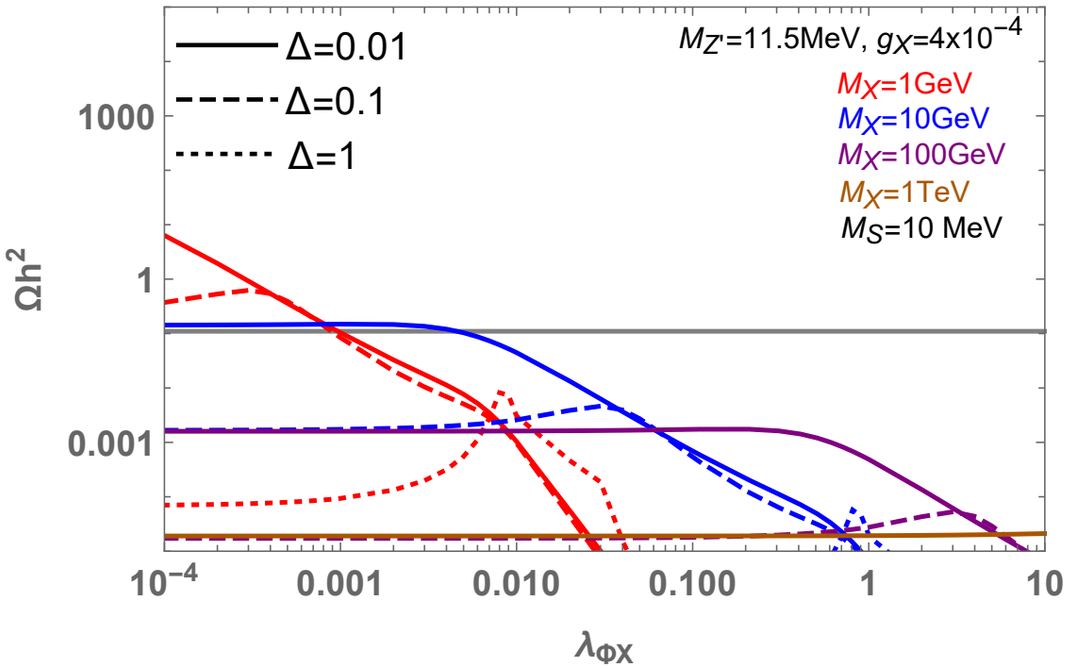

FIG. 5: Relic abundance of local Z_2 scalar DM. We take $\lambda_{XH} = 0$ for simplicity. (*Left*) We have used $M_{Z'} = 100\text{MeV}$ and $g_X = 8 \times 10^{-4}$ as inputs. (*Right*) Relic abundance of local Z_2 scalar DM. Here we used $M_{Z'} = 11.5\text{MeV}$ and $g_X = 4 \times 10^{-4}$ as inputs.

Complex Scalar DM:

$U(1)_{L_\mu - L_\tau} \to Z_3$ ($Q_\Phi = 3Q_X$)

Local Z_3 DM Model : first considered by Ko, Tang: arXiv:1402.6449 (SIDM), 1407.5492 (GC γ-ray excess)

$$V = -\mu_H^2 H^\dagger H + \lambda_H \left(H^\dagger H\right)^2 - \mu_\phi^2 \phi_X^\dagger \phi_X + \lambda_\phi \left(\phi_X^\dagger \phi_X\right)^2 + \mu_X^2 X^\dagger X + \lambda_X \left(X^\dagger X\right)^2$$
$$+ \lambda_{\phi H} \phi_X^\dagger \phi_X H^\dagger H + \lambda_{\phi X} X^\dagger X \phi_X^\dagger \phi_X + \lambda_{HX} X^\dagger X H^\dagger H + \left(\lambda_3 X^3 \phi_X^\dagger + H.c.\right) \quad (2.1)$$

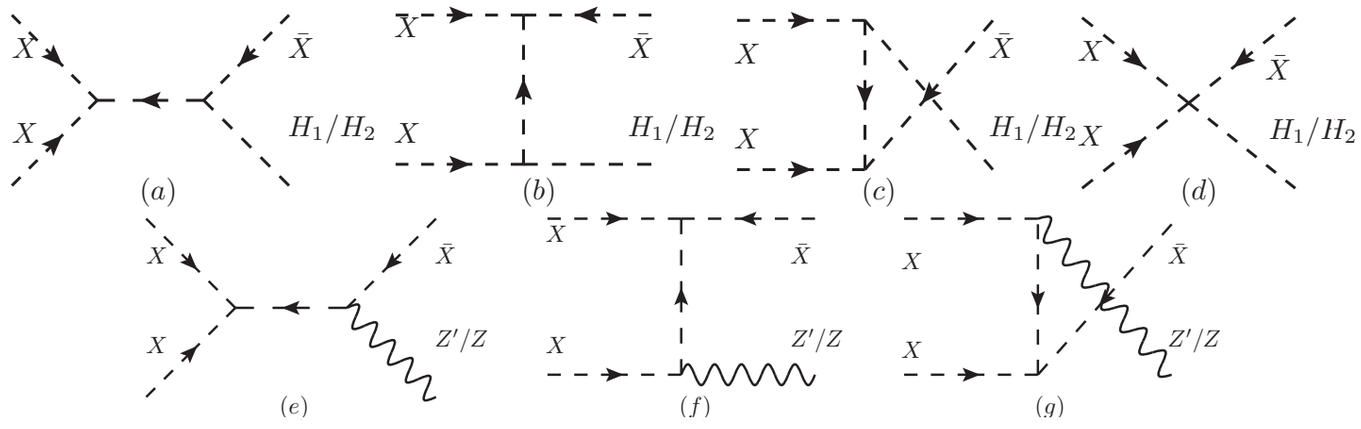

FIG. 1: Feynman diagrams for dark matter semi-annihilation. Only (a), (b), and (c) with H_1 as final state appear in the global Z_3 model, while all diagrams could contribute in local Z_3 model.

ϕ and Z' : present only in models with dark gauge symmetries, And not in models with global dark symmetries

Dark $U(1) \to Z_3$

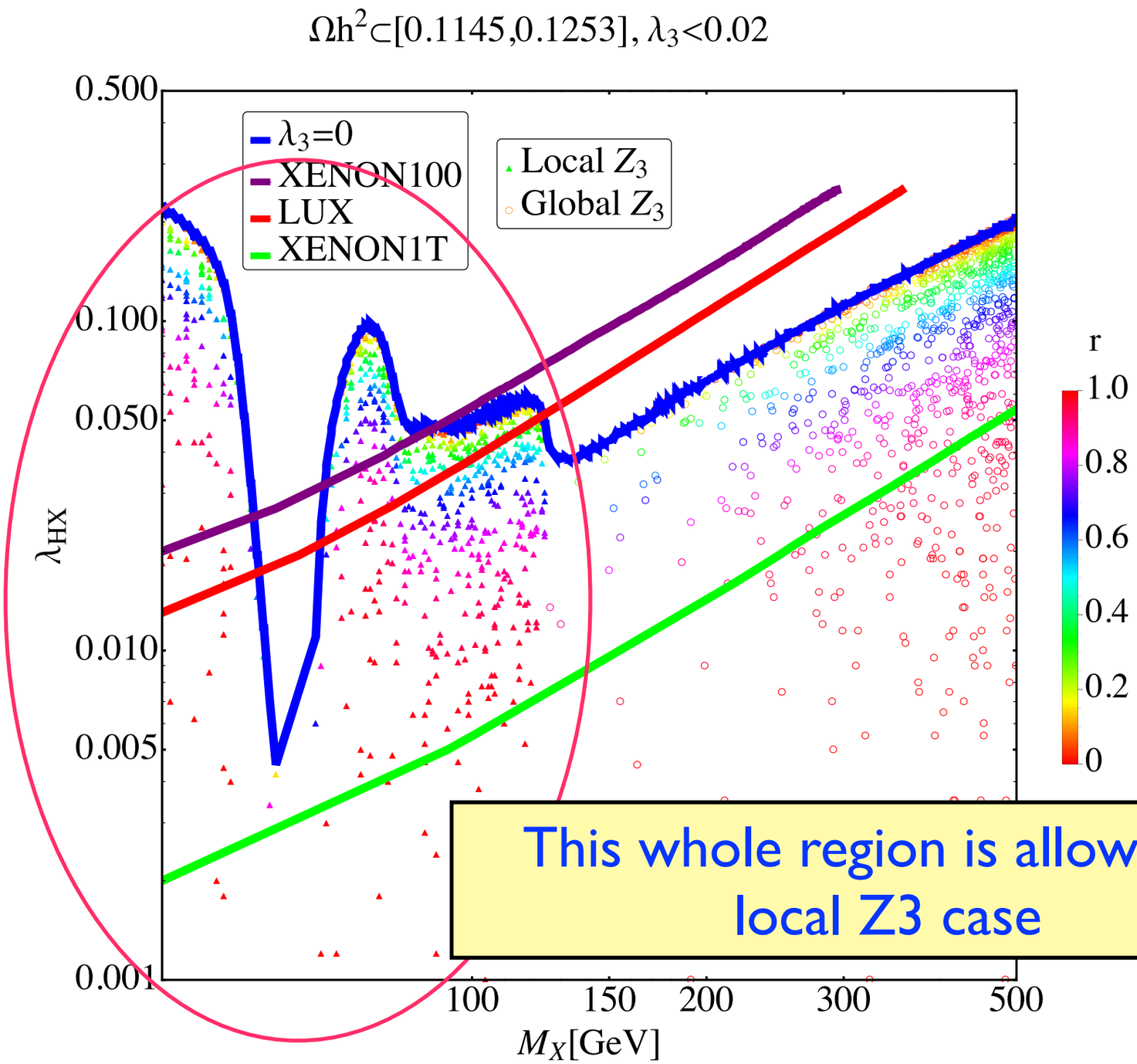

This whole region is allowed in local Z3 case

- Blue band marks the upper bound,
- All points are allowed in our local Z3 model,1402.6449
- only circles are allowed in global Z3 model,1211.1014

$$r \equiv \frac{1}{2} \frac{v\sigma^{XX \to X^* Y}}{v\sigma^{XX^* \to YY} + \frac{1}{2} v\sigma^{XX \to X^* Y}}.$$

$U(1)_{L_\mu - L_\tau} \to Z_3$

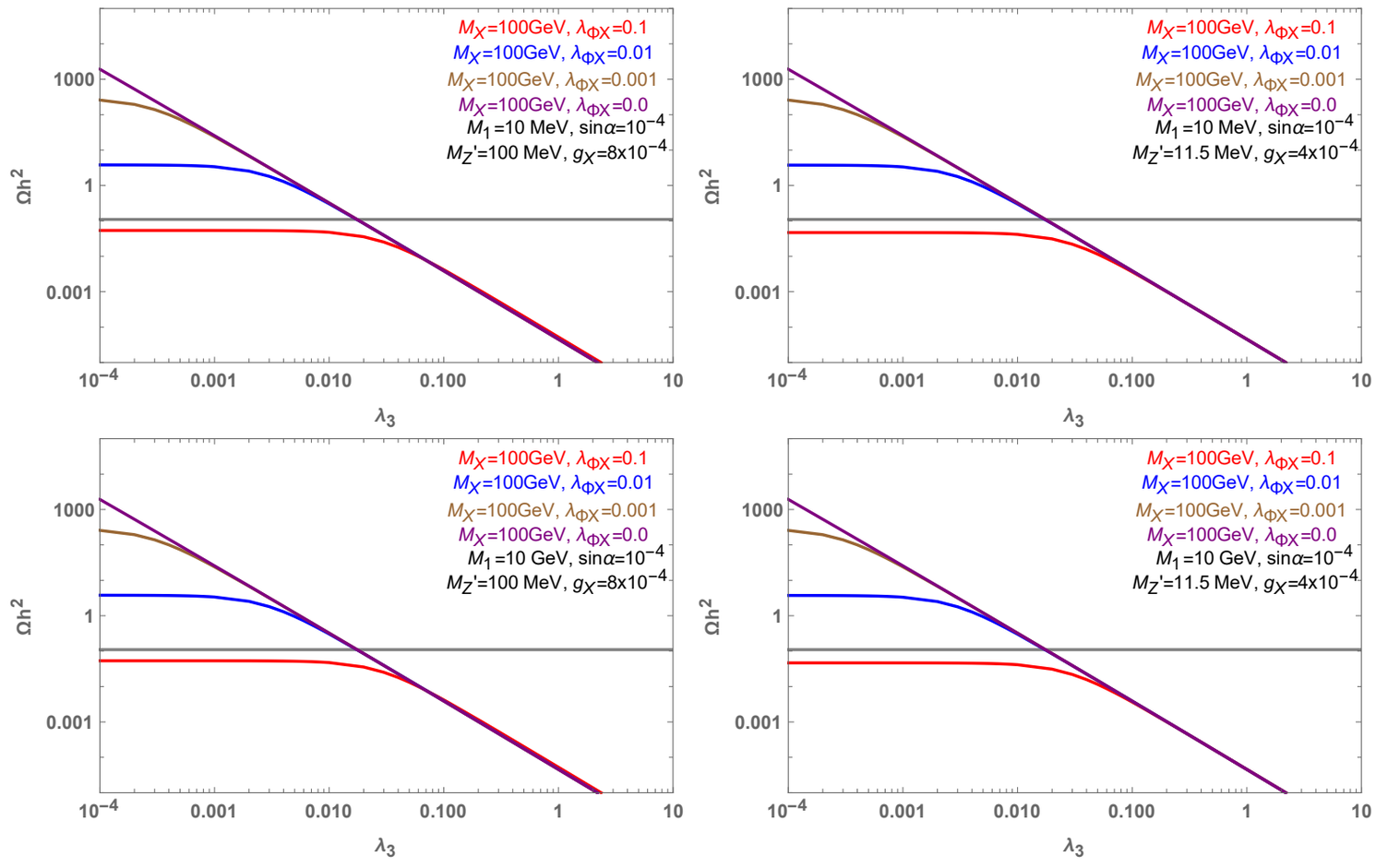

FIG. 6: Relic abundance of Z_3 scalar DM. We take $\lambda_{XH} = 0$ for simplicity. (*Left*) We have used $M_{Z'} = 100$MeV and $g_X = 8 \times 10^{-4}$ as inputs. (*Right*) Here we used $M_{Z'} = 11.5$MeV and $g_X = 4 \times 10^{-4}$ as inputs.

Dirac fermion DM:

$$U(1)_{L_\mu - L_\tau} \to Z_2 \; (Q_\Phi = 2Q_\chi)$$

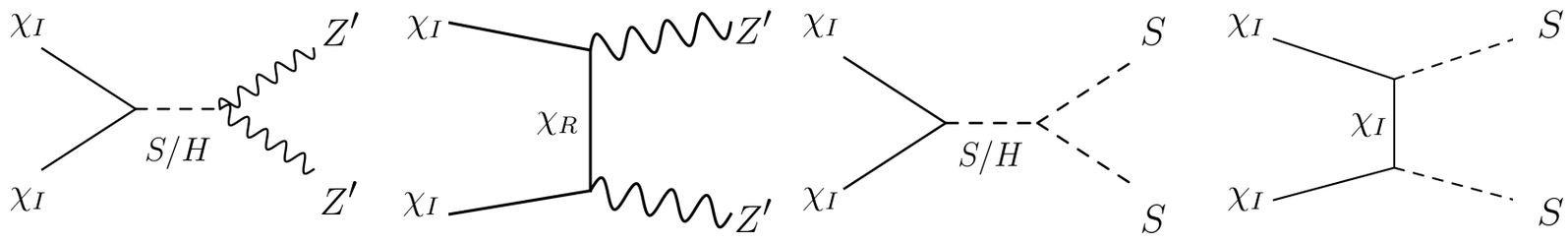

FIG. 8: (*Top*) Feynman diagrams of local Z_2 fermion DM annihilatiing to a pair of Z' bosons and S bosons, respectively. (*Bottom*) Feynman diagrams of local Z_2 fermion DM annihilatiing to Z' and S bosons.

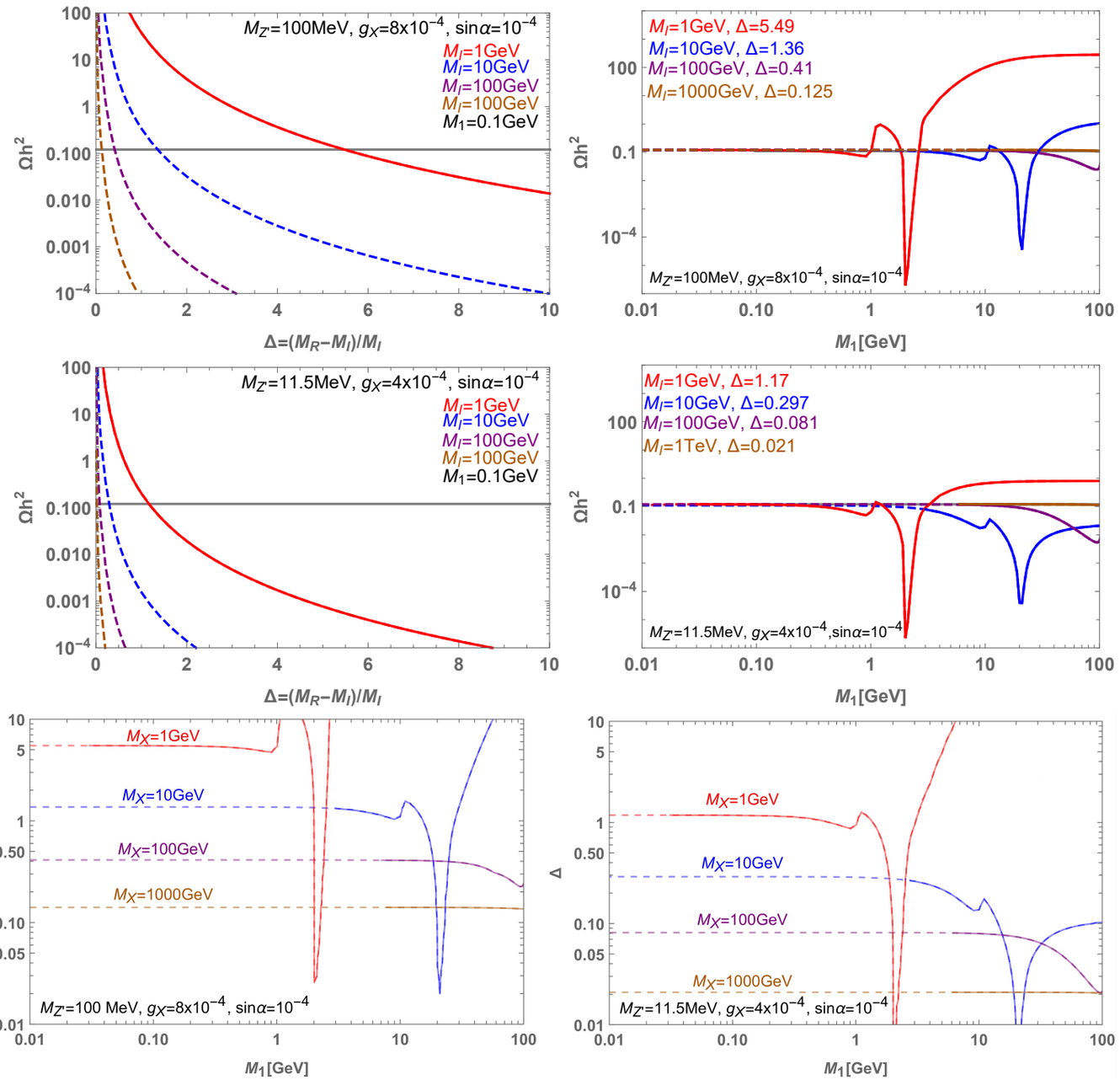

FIG. 8: The dark matter relic density as a function of mass difference between χ_R and χ_I or M_{H_1}. *(Top)* Here we used $M_{Z'} = 100$MeV and $g_X = 8 \times 10^{-4}$ as inputs. *(Middle)* Here we used $M_{Z'} = 11.5$MeV and $g_X = 4 \times 10^{-4}$ as inputs. *(Bottom)* Preferred paramater space in the $\Delta - M_1$ plane. Solid (Dashed) lines denote the region where bounds on DM direct detection are satisfied (ruled out).

Conclusion

- DM physics with massive dark photon is not complete without including dark gauge symmetry breaking Higgs field ϕ , which have been largely ignored by DM community

- Many examples showing the importance of ϕ

- Once ϕ is included, can accommodate the muon g-2 and thermal DM without the s-channel resonance condition $m_{Z'} \sim 2m_{\rm DM}$

- $m_{\rm DM}$: essentially free, whereas $m_{Z'} \sim O(10-100)$ MeV